Physics – Uspekhi **54** (7) 691 – 721 (2011)

REVIEWS OF TOPICAL PROBLEMS

PACS numbers: **36.40. – c**, 36.40.Sx, 61.43.Hv, 64.70.D–, 68.37.Hk

Processes involving clusters and small particles in a buffer gas

B M Smirnov

DOI: 10.3367/UFNe.0181.201107b.0713

Contents

Abstract. **Processes involving clusters and small particles are considered from the standpoint of interaction of clusters or small particles with atomic particles of a buffer gas. Two opposite interaction regimes are the kinetic (dynamic) and diffusion (hydrodynamic) ones, so that in the first case collisions of a gas atom with a cluster or small particle are analogous to collisions of two atomic particles in a gas, whereas in the diffusion regime a cluster or a small particle strongly interacts simultaneously with many atoms. Criteria and parameters of processes for the kinetic and diffusion regimes are given for transport phenomena in gases involving clusters or small particles, cluster charging in an ionized gas and particle combustion, and also nucleation processes including cluster growth as a result of atom attachment to a growing cluster, the coagulation and coalescence processes.**

B M Smirnov Joint Institute for High Temperatures,
Russian Academy of Sciences,
ul. Izhorskaya 13/19, 125412 Moscow, Russian Federation
Tel./Fax (7-499) 190 42 44
E-mail: bmsmirnov@gmail.com

Received 21 October 2010, revised 11 January 2011
Uspekhi Fizicheskikh Nauk **181** (7) 713 – 745 (2011)
DOI: 10.3367/UFNr.0181.201107b.0713
Translated by B M Smirnov; edited by A Radzig

1. Introduction

Rates of processes involving clusters are of great interest for gases and plasmas containing clusters or small particles. Let us consider as an example cluster motion in a gas and ascertain its character. Until the cluster is small, its collisions with gas atoms proceed analogously to collisions of atomic particles in a gas, so that at each instant of time the cluster may strongly interact with only one atom or molecule. Cluster kinetic parameters are determined then by analogy with such parameters of atomic particles in a gas, where they are expressed through the cross sections of atomic particle collisions with gas atoms or molecules. In contrast, the diffusion regime of cluster transport takes place at a large cluster size, where many gas atoms or molecules collide with the cluster simultaneously, and cluster motion is governed by hydrodynamic laws. The goal of this paper is to analyze the kinetic and diffusion regimes of various cluster processes in a gas. It would seem that if the mean free path of gas atoms or molecules is large compared to the cluster size, the kinetic regime of cluster processes is realized, whereas the opposite relation between these parameters leads to the diffusion regime of cluster processes. But a more detailed analysis shows that it is not always correct, and we will demonstrate this below.

Let us consider physical objects and systems where processes involving cluster transport in a gas are of interest. First, this is a cluster plasma formed in the generation of cluster beams from laser action on a surface [1–5], on the basis of magnetron [6–11] or arc [12, 13] plasmas, or as a result of

free jet expansion [14–19]. In particular, laser irradiation of a metal surface leads to the generation of an atomic flux whose parameters are varied in the course of its passage through a buffer gas. The size distribution function of clusters formed from the atomic flux is determined by these parameters. Second, processes involving clusters and small particles are of importance for power plants which use the combustion of a solid organic fuel, where soot and other small particles are present in gaseous products. Two methods are employed in order to remove these particles from the gas stream, so that in the first one particles are charged and removed from the stream by electric field action. The second method uses the inertia of particles at hand, which is high compared to that of gas atoms or molecules because of their large mass. Therefore, if a gas stream is turned about in so-called impactors [20, 21], particles continue their straightforward motion, and in this manner may be removed from the gas stream. Of course, the first method has been studied well enough and also includes charging of particles and their precipitation in an electric field [22–24]. These methods have been used in power plants for many decades, but the further development of the power industry raises new problems and requires more detailed understanding of the processes in a gas containing small particles. Third, the processes under consideration are of importance in the combustion of powders and metals because molecules of oxides resulting from these processes form strong chemical bonds among themselves and join into small particles. The growth rates of such particles are different in the kinetic and diffusion regimes of particle transport, and the criteria of each regime are required in the analysis of particle growth.

The above laboratory gaseous systems with clusters or small particles may be added by corresponding natural systems. An example of this is a solar dusty plasma resulting from interaction of the solar wind with a dust evaporated from the surface of a planet satellite. This plasma creates, in particular, Saturn's and Jupiter's rings, but the magnetic fields of these planets and their interaction with fields of the solar wind are more important for ring formation. These issues are outside our consideration, and in the analysis of the above objects we will restrict ourselves to the interaction of single dust particles with a surrounding plasma. One more bunch of questions connected with this topic relates to aerosol behavior in Earth's atmosphere, where the processes involving aerosols and small particles depend significantly on the local parameters of the atmosphere and particles, including their chemical compositions.

The processes under consideration are analogous to those in colloid solutions and processes involving biological clusters [25]; nevertheless, below we restrict ourself to gaseous systems only. Single clusters or small particles nanometers and micrometers in size located in a gas or plasma are the object of our consideration. Probes [26, 27] are not included in this list, though their size of 50–400 μm [28] corresponds to the boundary of the indicated range, since probes cannot be considered as free particles in a gas. The size of artificial satellites and asteroids [29, 30] is outside the indicated range, and hence the behavior of these objects is governed by other processes. Note that our analysis is based on old concepts (see, for example, book [31]) which arose in the consideration of other physical objects. Therefore, the goal of this paper is not a new look at some aspects of cluster physics and the physics of small particles, but the analysis of processes involving clusters and small particles from the standpoint of the influence of gas on the character of these processes.

The processes proceeding with participation of clusters and small particles in gases may be separated into three groups. The transport processes of clusters or small particles in gases, including diffusion and mobility of clusters and small particles in gases, their relaxation in gaseous flows, etc. are regarded as processes of the first group. Transition from the kinetic regime to the diffusion (or hydrodynamic) one occurs if the mean free path of gas atoms or molecules is comparable to the cluster size. Attachment processes of atomic particles located in a buffer gas to clusters are related to processes of the second group. These processes include quenching of excited atomic particles located in a gas on the surface of clusters or small particles, chemical processes, including combustion, on the cluster surface involving active molecules, particularly if this cluster is a fuel and the surrounding gas contains oxygen. The processes of charging a small particle in an ionized gas as a result of attachment of electrons or ions from a surrounding gas and their subsequent recombination on the particle surface are related to this group. Then, the criterion of transition from the kinetic regime to the diffusion one is determined by the character of motion for a cluster-attaching atomic particle in a gas. Here, not only the range of action of the cluster or small particle field but also the concentration of attaching atomic particles may exert some influence on this criterion. The third group includes processes for the growth of clusters and small particles in a buffer gas. Note that in the case of coagulation — the joining of liquid clusters at their contact — and the growth of fractal structures as a result of joining fractal aggregates, the criterion of transition from the kinetic regime of aggregation to the diffusion one, along with the relation between the mean free path of fragments in a buffer gas and their sizes, also includes the relation between these size parameters and the mean distance between fragments in a buffer gas.

In all the cases of collisions between atomic particles and a cluster surface, we assume the cluster to have a spherical shape and a hard surface. This means that the region of the cluster's strong interaction with an atomic particle is small compared to cluster size and such an assumption is fulfilled for large clusters because the radius of the cluster's strong interaction with an atomic particle is on the order of atomic size. But the hard sphere model is also valid for thermal collisions of atoms and molecules [32] (this means that the scattering is determined mostly by repulsive interaction), so that the assumption of a hard cluster boundary holds true for small clusters consisting of a small number of atoms, though it requires the attraction of additional parameters of interaction. As for the assumption that the cluster has a spherical shape, it corresponds to some averaging. The experience of cluster analysis shows that the accuracy in the analysis of collisions between a cluster and an atomic particle is determined not by errors in the model used, but by the accuracy and the availability of the additional parameters of atom–cluster interaction. This justifies the model of the spherical cluster shape with a hard surface for the analysis of collision processes between atomic particles and clusters. Within the framework of this model, the difference between clusters and small particles is lost, and below we will use the term 'cluster' not only for nanoclusters, but also for microparticles.

Note that the goal of this review is to give simple algorithms for the determination of the rate constants of

processes involving clusters and small particles, along with the criteria where this is valid. The author hopes that this consideration will allow the reader to obtain numerical results for the rates of certain processes under given conditions.

2. Models of clusters and processes involving their participation

2.1 Cluster structure and properties

Clusters as systems consisting of a finite number of bound atoms are a specific physical object due to the magic numbers of solid clusters [33]. This means that some cluster parameters, such as the binding energy of a surface atom, the cluster ionization potential, or the cluster electron affinity, have extrema at magic numbers of cluster atoms. In reality, the magic numbers of cluster atoms correspond to completed cluster structures or to filled electron shells. Therefore, clusters with magic numbers of atoms are formed in gases more effectively than clusters with neighboring numbers of atoms. Correspondingly, clusters with magic numbers of atoms are observed as local maxima in mass spectra of clusters produced in cluster beams or in gases [34] and in mass spectra of cluster beam photoionization [35]. Magic numbers of cluster atoms are observed in experiments involving up to tens of thousands of cluster atoms [36].

Based on the above cluster properties, one can analyze clusters by numerical simulation methods. Setting aside problems with computer methods connected with finding parameters of atomic interactions, we aim to validate simple and universal methods which do not take into account certain cluster structures. Therefore, we determine first the accuracy of analytical universal cluster models. The strongest nonmonotonity in cluster parameters as a function of the number of cluster atoms relates to parameters of the phase transition, and Fig. 1 gives the dependence of the melting point of sodium clusters on the number of cluster atoms [37, 38]. As is seen, values of the melting points are scattered roughly within the limits of 20%. For other parameters of clusters and processes, the range of nonregularity is more narrow. If we draw a monotonic dependence on the basis of the data of Fig. 1, we obtain a 10% error in the melting points for clusters of a certain size. From this reasoning, we will accept below that the application of regular models for clusters some nanometers in size, as in Fig. 1, leads to an error of 10%.

Let us now ascertain the potential of computer models in cluster analysis. Note that computer models are vitally important for cluster physics, especially for describing cluster properties which are determined by the simultaneous interaction of many atoms, where one-particle models are not valid. The behavior of the potential energy surface is essential for cluster behavior, because in the many-dimensional space of atomic coordinates the potential energy surface has many local minima [39–41]. From this it follows that any system of bound classical atoms has many stable atomic configurations, and the dynamics of cluster evolution consist in transitions between neighboring local minima of the potential energy surface through potential barriers [42, 43]. Hence, cluster evolution results from a sequence of transitions between local minima of the potential energy surface [44, 45]. Another principal cluster property discovered in computer cluster simulations by methods of molecular dynamics is the phase coexistence near the phase transition point [46–48]. The latter

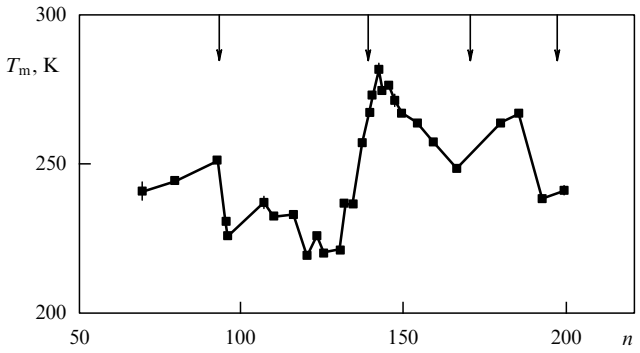

Figure 1. Dependence of the melting point T_m of sodium clusters on the number of atoms n in the cluster [37, 38]. The melting point of bulk sodium amounts to 301 K.

is a general property of a system of a finite number of bound particles.

Let us consider the possibilities of cluster computer simulation where cluster parameters depend on the interaction between individual atoms. This problem is reliably solved in the case of the pair interaction of cluster atoms, as takes place in inert gas clusters. But for metal clusters, however, which are the subject of consideration in this review, the choice of interaction is not unambiguous, and even the atomic configuration for the ground state of clusters may be different depending of the interaction model (see, for example, Ref. [49]). Therefore, computer simulation of isolated clusters depends on information about the parameters of interaction inside the cluster, and usually available information does not allow us to use the potential of computer methods in full measure, especially for processes involving clusters. We will apply below simpler, but more reliable, analytical methods in the analysis of cluster processes.

2.2 Liquid drop model

Within the liquid drop model that we will use below, a cluster is modelled by a spherical liquid drop where individual atoms are modelled by noncompressed liquid drops. The liquid drop model is the simplest and most practical model [50] having a universal character and has been utilized for various physical objects. This model was introduced in nuclear physics by Niels Bohr [51] and allowed one to analyze various properties of an atomic nucleus [52–54]. Namely this model, but not more accurate ones, explained at that time the possibility of atomic nucleus fusion [55].

Evidently, a cluster is a simpler physical object in comparison to an atomic nucleus consisting of particles of two kinds. One can reduce interaction inside a cluster to electrostatic interaction between cluster atoms or ions and to exchange interaction (electron–electron interaction), and then the distance between neighboring atoms or ions is determined by competition among these interactions. We use the fact that the same takes place for macroscopic systems of bound atoms [56, 57], which allows us to express the parameters of the liquid drop model through the parameters of a bulk atomic system. Let us introduce the Wigner–Seitz radius r_W [56, 57], so that the number n of cluster atoms in a cluster of radius r_0 is given by the expression

$$n = \left(\frac{r_0}{r_W}\right)^3 . \qquad (2.1)$$

Table 1. Parameters of some metals and semiconductors: ρ is the material density at the melting point or at room temperature, r_W is the Wigner–Seitz radius.

Element	ρ, g cm^{-3}	r_W, Å	Element	ρ, g cm^{-3}	r_W, Å	Element	ρ, g cm^{-3}	r_W, Å
Li	0.512	1.71	Zn	6.57	1.58	La	5.94	2.10
Be	1.69	1.28	Ga	6.08	1.66	Hf	12	1.81
Na	0.927	2.14	Rb	1.46	2.85	Ta	15	1.68
Mg	1.584	1.82	Sr	6.98	1.71	W	17.6	1.61
Al	2.375	1.65	Zr	5.8	1.84	Re	18.9	1.58
K	0.828	2.65	Mo	9.33	1.60	Os	20	1.56
Ca	1.378	2.26	Rh	10.7	1.56	Ir	19	1.59
Sc	2.80	1.85	Pd	10.4	1.60	Pt	19.8	1.57
Ti	4.11	1.66	Ag	9.32	1.66	Au	17.3	1.65
V	5.5	1.54	Cd	8.00	1.77	Hg	13.6	1.80
Cr	6.3	1.48	In	7.02	1.86	Tl	11.2	1.93
Fe	6.98	1.47	Sn	6.99	1.89	Pb	10.7	1.97
Co	7.75	1.44	Sb	6.53	1.95	Bi	10.0	2.02
Ni	7.81	1.44	Cs	1.843	3.06	U	17.3	1.77
Cu	8.02	1.47	Ba	3.34	2.54	Pu	16.7	1.70

The Wigner–Seitz radius is expressed through the density ρ of the macroscopic system as

$$r_W = \left(\frac{3m_a}{4\pi\rho}\right)^{1/3}, \tag{2.2}$$

where m_a is the mass of the atom. The Wigner–Seitz radius represents the fundamental parameter of cluster physics, and its values are given in Table 1 [31, 58] for the density of the liquid bulk system at the melting point or, if such information is absent, at room temperature. The above definition (2.2) for the Wigner–Seitz radius may also be used for molecular clusters. It should be noted that in the model employed we assume the Wigner–Seitz radius to be independent both of the cluster temperature and of the cluster aggregate state. This assumption leads to an error in the parameters of the processes under consideration of about several percent. Note that within the framework of the liquid drop model no distinction between a nanocluster and microparticle is made, so the subsequent analysis relates equally to both objects, though we will often use the term 'cluster'.

The existence of magic numbers of cluster atoms for solid clusters leads to a nonmonotonic dependence of cluster parameters on the number of cluster atoms. Nevertheless, it is convenient to use models with such monotonic dependences that correspond to averaging over cluster structures in some range of cluster sizes. The liquid drop model is a continuous model for cluster parameters and it considers a cluster to be cut out of a liquid bulk atomic system. In the case of a liquid cluster, averaging over cluster structures proceeds automatically for each cluster of a given size.

2.3 Hard sphere model for processes involving clusters

We will use as our base the hard sphere model in the analysis of the dynamics of processes involving clusters. This means that the interaction potential of colliding particles, say, a cluster and an atom, is taken in the form

$$U(R) = 0\,,\ r > R_0\,;\quad U(R) = \infty\,,\quad r < R_0\,, \tag{2.3}$$

where R is the distance between colliding particles, and R_0 is the hard sphere radius which is equal to the sum of radii of colliding particles. Though the hard sphere model is analogous to the above liquid drop model, they relate to different kinds of particles. Indeed, the liquid drop model describes statistical cluster properties where the cluster consists of hard balls, while the hard sphere model relates to the collision dynamics of particles with a repulsive interaction potential between them, and this interaction potential varies sharply with variations of the distances between particles in a range that is responsible for particle scattering. Next, if we introduce the interaction potential of constituent particles in the liquid drop model, it is necessary to add to the interaction potential (2.3) a narrow well at $R = R_0$, which is responsible for the formation of a bound state of colliding particles.

The hard sphere model has a long history, starting from Maxwell's investigations [60–62], where molecular collisions were considered like collisions of billiard balls. This allowed him to find the velocity distribution function for an ensemble of free molecules (the Maxwell distribution) and to analyze the transport phenomena in this system. This model has a universal character and may be applied to the analysis of various systems and processes. In this context, we mention investigations of thermodynamic properties for systems of many particles, including the liquid aggregate state of a particle ensemble [63, 64]. In the analysis of atom–cluster collisions, we note that the range of their strong interaction is on the order of the atomic size and corresponds to the atom's location near the cluster surface. Therefore, the hard sphere model is justified for the collision of an atom with a large cluster that consists of a great many atoms. Thus, skipping the details of collision dynamics, we find that the diffusion cross section of atom–cluster collisions is independent of the collision velocity and is given by

$$\sigma^* = \pi r_0^2\,, \tag{2.4}$$

where r_0 is a cluster radius, and the inequality $r_0 \gg a_0$ holds true, with a_0 being the Bohr radius. The same expression relates to the hard sphere model that is based on a sharp dependence of the interaction potential on the distance between colliding particles. This model also describes the interaction and collision of gaseous atoms and molecules, and Table 2 contains the gas-kinetic cross sections for collisions of gaseous atoms and molecules, which are the average diffusion cross sections for collisions of atomic particles at room temperature.

If we assume that an atom–cluster contact in the course of their collision leads to attachment of the atom to the cluster

Table 2. Gas-kinetic cross sections σ_g for collisions of atoms and molecules, expressed in 10^{-15} cm^2 [59].

Colliding particles	He	Ne	Ar	Kr	Xe	H_2	N_2	O_2	CO	CO_2
He	1.3	1.5	2.1	2.4	2.7	1.7	2.3	2.2	2.2	2.7
Ne		1.8	2.6	3.0	3.3	2.0	2.4	2.5	2.7	3.1
Ar			3.7	4.2	5.0	2.7	3.8	3.9	4.0	4.4
Kr				4.8	5.7	3.2	4.4	4.3	4.4	4.9
Xe					6.8	3.7	5.0	5.2	5.0	6.1
H_2						2.0	2.8	2.7	2.9	3.4
N_2							3.9	3.8	3.7	4.9
O_2								3.8	3.7	4.4
CO									4.0	4.9
CO_2										7.5

surface, with the subsequent release of the atom at the isotropic atomic distribution over the angles of scattering, we obtain the following expression for the rate constant of atomic scattering:

$$k = v_T \sigma^* = k_0 n^{2/3}, \quad k_0 = \sqrt{\frac{8T\pi}{m_a}} r_W^2, \tag{2.5}$$

where T is the gas temperature expressed in energy units, m_a is the atomic mass, $v_T = \sqrt{8T/\pi m_a}$ is the thermal atomic velocity, and n is the number of cluster atoms. Table 3 contains values of the reduced rate constant of atomic scattering at the temperature of 1000 K [58, 12]. The reduced parameters of atom–cluster collisions may be used for the quantitative analysis of cluster processes.

Let us consider the rate constant of a contact between two colliding clusters within the framework of the hard sphere model. This contact may be an intermediate stage of other processes, in particular, the process of cluster joining. Since the cross section of cluster collisions for the hard sphere model is defined as $\sigma = \pi(r_1 + r_2)^2$, where r_1, r_2 are radii of colliding clusters, we have for the rate constant of this process [12] the following expression

$$k(n_1, n_2) = \langle v\, \pi(r_1 + r_2)^2 \rangle = \sqrt{\frac{8T}{\pi\mu}} \pi (r_1 + r_2)^2 = k_0 \sqrt{\frac{n_1 + n_2}{n_1 n_2}} \left(n_1^{1/3} + n_2^{1/3}\right)^2, \tag{2.6}$$

where μ is the reduced mass of colliding clusters, and the reduced rate constant k_0 of cluster collisions is given by formula (2.5). Since the rate constant $k(n_1, n_2)$ is symmetric with respect to permutation $n_1 \leftrightarrow n_2$ and depends weakly on a number of cluster atoms, it is convenient to approximate this quantity by the dependence

$$k(n_1, n_2) = 5k_0 (n_1 + n_2)^{1/6}, \tag{2.7}$$

and the numerical coefficient used corresponds to identical sizes of colliding clusters: $n_1 = n_2$. In the case of $n_1/n_2 = 1.5$, the numerical coefficient equals 5.1, and in the case of $n_1/n_2 = 2$ it is equal to 5.2, so that the accuracy of the used approximation is several percent.

In the above cases, an atom–cluster contact or a contact between two colliding clusters results from the free motion of particles. However, the approach of two particles in a dense buffer gas may be restricted by their collisions with buffer gas atoms, and we will determine below the rate of this process if the diffusion motion of the particles in the buffer gas determines their approach. The flux of admixture atoms to the cluster surface is given by $j = -D_m \nabla N_m$ for the diffusion character of atom attachment to the cluster surface, where D_m is the diffusion coefficient in a buffer gas for admixture atoms which constitute the cluster, and N_m is the number density of these atoms in a buffer gas. Correspondingly, for the total number J of admixture atoms which intersect a sphere of radius R per unit time and subsequently attach to the cluster we have the following expression

$$J = 4\pi R^2 D_m \frac{dN_m}{dR}.$$

Because of the conservation of the total number of attaching atoms outside the cluster, the quantity J is independent of sphere radius R, and the above relation may be used as the equation for $N_m(R)$. Solving this equation with the boundary

Table 3. The reduced rate constant k_0 for a cluster collision with a parent atom in accordance with formula (2.5) at the temperature of 1000 K.

Element	k_0, 10^{-11} cm^3 s^{-1}	Element	k_0, 10^{-11} cm^3 s^{-1}	Element	k_0, 10^{-11} cm^3 s^{-1}	Element	k_0, 10^{-11} cm^3 s^{-1}
Li	17	Ga	4.8	La	5.4	Ta	3.0
Be	7.9	Ge	4.5	Hf	3.5	W	3.6
Na	14	Rb	13	Ce	5.1	Re	2.7
Mg	9.8	Sr	4.5	Pr	5.1	Os	2.6
Al	7.6	Zr	5.1	Nd	4.9	Ir	2.6
K	16	Nb	4.3	Pm	4.8	Pt	2.6
Ca	12	Mo	3.8	Sm	4.7	Au	2.8
Sc	7.4	Rh	3.8	Eu	6.1	Hg	3.3
Ti	5.8	Pd	3.5	Gd	4.8	Tl	3.8
V	4.8	Ag	3.8	Tb	4.7	Pb	3.9
Cr	4.4	Cd	4.3	Dy	4.4	Bi	4.1
Fe	4.2	In	4.7	Ho	4.4	Th	3.8
Co	3.9	Sn	4.7	Er	4.3	U	2.9
Ni	3.9	Sb	5.0	Tm	4.4	Pu	2.9
Cu	4.2	Cs	12	Yb	5.4	—	—
Zn	4.5	Ba	7.9	Lu	4.2	—	—

condition $N_m(r_0) = 0$, we obtain

$$N_m(R) = \int_{r_0}^{\infty} \frac{J\,dR}{4\pi R^2 D_m} = \frac{J}{4\pi D_m}\left(\frac{1}{r_0} - \frac{1}{R}\right).$$

Denoting the number density of admixture atoms far from the cluster by N_m, we arrive at the Smoluchowski formula [74] for the rate of cluster growth:

$$J = 4\pi D_m r_0 N_m\,. \tag{2.8}$$

One can generalize this formula to the case where the joining of two clusters proceeds as the result of their diffusion motion in the buffer gas. Then, the rate constant of joining the two clusters can be written as

$$k_{12} = 4\pi(D_1 + D_2)(r_1 + r_2)\,, \tag{2.9}$$

where D_1, D_2 are the diffusion coefficients of colliding clusters in a buffer gas, and r_1, r_2 are the cluster radii.

2.4 Analytical and computer methods in cluster physics

Summing up the above analysis in Sections 2.2, 2.3, we note that only a restricted circle of processes involving clusters and small particles in gases and plasma was considered, and they are of concern in practical applications. Though the range of these issues may be widened, the above analysis can provide possible theoretical grounds for examining these problems. The basis of this analysis comprises concepts introduced in physics many years ago, in any case before the creation of such new areas of physics as cluster plasma and dusty plasma, which concern the topic under consideration, i.e., the behavior of isolated clusters or small particles in a buffer gas or plasma. For this reason, the material represented is mostly a methodical in character. Next, we utilized only two simple models, namely, the liquid drop model for the cluster structure, and the hard sphere model in the analysis of the collision processes involving clusters. The accuracy of the parameters for the processes under consideration is estimated as 10–20%. The advantage of analytical methods consists in the possibility of using analytical formulas for the rate constants of cluster processes with reliable parameters for certain particles and processes. It is impossible, however, to improve the accuracy of the results within the framework of analytical methods, whereas computer methods allow us to do this, in principle. Below, we will compare the analytical approach and computer simulation for a simple example.

Let us consider the collision of a metal atom with a cluster consisting of atoms of the same sort. In accordance with the position of this paper, we are based on the liquid drop model for the cluster, and its radius r_0 is then given by formula (2.1), where r_W is the Wigner–Seitz radius introduced according to formula (2.2). Correspondingly, the diffusion cross section for atom–cluster scattering is πR_0^2 within the framework of the hard sphere model, and the hard sphere radius is defined as $R_0 = r_0 + r_W$. We will use this formula in subsequent expressions for transport coefficients. Let us now formulate the algorithm for the solution of this problem in computer simulation. We first choose an appropriate interaction pattern inside the cluster. For example, the cluster potential energy can be represented as a sum of the pair interaction potentials in the Sutton–Chen form [66], where the pair interaction potential includes electrostatic and exchange interactions, or is taken in the form of the tight-binding scheme [67, 68], where exchange interaction of atomic cores and electrons is added to a repulsive interaction potential of atomic cores. In both cases, clearly, the computer method takes in at least two parameters of the potential energy (for example, the potential well depth and the distance between nearest neighbors for pair interaction), and these parameters follow from comparing measured parameters of the bulk metal with those calculated within the framework of the computer approach. We note that this simple algorithm of computer simulation of intercluster and atom–cluster interactions holds true for the classical character of atomic motion. The latter is not valid for electrons, and then the density functional theory [69, 70] is used for describing the spatial electron distribution function. As is seen, the above algorithm for computer simulation does not differ, in principle, from the analytical method based on the liquid drop model or the hard sphere model for processes involving clusters. The analytical method employs one interaction parameter, the Wigner–Seitz radius. Generally, computer simulation can provide a higher accuracy because it uses a larger number of interaction parameters, but the numerical simulation requires a more detailed analysis of interaction inside the cluster and does not have a universal character, i.e., each computer evaluation relates to a certain cluster system. In addition, a formal usage of computer methods without a special analysis of the introduced parameters may lead to unreliable results. It should also be noted that the range of processes under consideration does not include many problems of cluster physics (see, for example, Refs [71–73]).

3. Clusters in transport phenomena in gases

3.1 Cluster motion in gas in an external field

The transport of clusters in a gas is determined by their interaction with gaseous atoms or molecules, and this interaction is different depending on the gas density and cluster size. In a rarefied gas, the braking force for a moving cluster results from single atom–cluster collisions that correspond to the kinetic regime of the cluster transport in a gas. In a dense gas, many atoms interact with the cluster at each time, and the character of cluster motion in a gas has a hydrodynamical character. This motion is similar to that of a macroscopic particle located in a dense gas or liquid. These two mechanisms of atom–cluster interaction are demonstrated in Fig. 2.

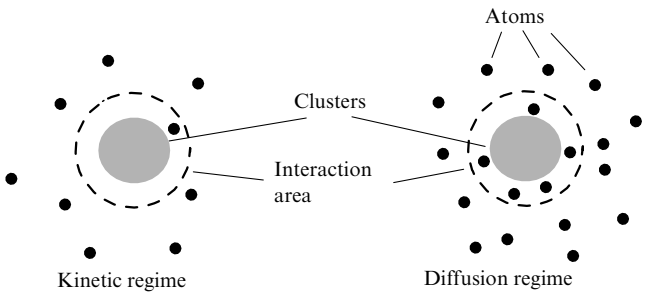

Figure 2. Character of cluster interaction with surrounding atoms in the course of cluster motion in a buffer gas. For the kinetic regime of cluster interaction with a buffer gas, only one atom or molecule may strongly interact with the cluster at each instant of time, while in the diffusion regime many atoms interact simultaneously with the cluster.

The braking force acting on a cluster which moves in a rarefied gas with velocity $\mathbf{w}$ and resulting from collisions with buffer gas atoms is defined as

$$\mathbf{F}_{\rm kin} = \int m(\mathbf{v}-\mathbf{w})(1-\cos\vartheta)\,\varphi(v)\,g\,{\rm d}\sigma\,{\rm d}\mathbf{v}\,.$$

Here, $\mathrm{d}\sigma$ is the differential cross section of atom scattering on a cluster, so that ϑ is the scattering angle, g is the relative velocity of particles, and $\varphi(v)$ is the velocity distribution function of atoms that is normalized to the number density $N_{\rm a}$ of gas atoms, i.e., $\int \varphi(v)\,{\rm d}\mathbf{v} = N_{\rm a}$. The Maxwell distribution function of atoms over velocities has the form

$$\varphi(v) = N_{\rm a}\left(\frac{m}{2\pi T}\right)^{3/2}\exp\left(-\frac{mv^2}{2T}\right),$$

where m is the gaseous atom mass, and T is the gas temperature expressed in energy units. For an atom–cluster collision within the framework of the hard sphere model, the above expression for the braking force acting on the cluster is simplified (see, for example, Refs [31, 58, 77]):

$$\mathbf{F} = -\mathbf{w}\,\frac{8\sqrt{2\pi mT}}{3}\,N_{\rm a}r_0^2\,. \tag{3.1}$$

The minus sign accounts for the direction of the braking force opposite to the cluster motion. Evidently, this formula holds true in the limit $\lambda \gg r_0$, where λ is the mean free path of atoms in the buffer gas. Indeed, the Maxwell distribution function of atoms over velocities is violated near the cluster at a distance on the order of λ from it. Therefore, if a region occupied by a cluster is small compared to the mean free path of atoms, the distortion of the Maxwell distribution function of atoms due to collisions with the cluster is not essential.

In another limiting case (diffusion regime), the braking force acting on a cluster that moves in a gas with velocity w is given by the Stokes formula [78, 79]

$$F_{\rm St} = 6\pi\eta r_0 w, \quad \lambda \ll r_0\,, \tag{3.2}$$

where η is the gas viscosity. Within the framework of the hard sphere model, the mean free path λ of gas atoms is defined as $\lambda = (N_{\rm a}\sigma_{\rm g})^{-1}$, where $\sigma_{\rm g} = \pi\rho_0^2$ is the gas-kinetic cross section of atomic collisions, i.e., the average diffusion cross section for collisions of gas atoms at room temperature, so that ρ_0 is the effective radius of atomic interaction, and this cross section is assumed to be independent of the temperature. In the first Chapman–Enskog approximation [75, 76], the gas viscosity takes the form

$$\eta = \frac{5\sqrt{\pi Tm}}{24\sigma_{\rm g}} = \frac{5\sqrt{Tm}}{24\sqrt{\pi}\rho_0^2}\,. \tag{3.3}$$

Using the above formulas (3.3), we find for the ratio of friction forces in the kinetic (3.1) and diffusion (3.2) regimes:

$$\frac{F_{\rm kin}}{F_{\rm St}} = \frac{15\pi}{32\sqrt{2}}\,\frac{\lambda}{r_0} = 0.96\,{\rm Kn}\,, \tag{3.4}$$

where ${\rm Kn} = \lambda/r_0$ is the Knudsen number, and the mean free path of atoms in the gas is $\lambda = (N_{\rm a}\sigma_{\rm g})^{-1}$. As is seen, the cluster braking regime depends on the ratio between parameters λ and r_0. Thus, there is a continuous transition from the kinetic regime of cluster interaction with a buffer gas to the diffusion regime as the number density $N_{\rm a}$ of atoms or the cluster radius r_0 increases, and this transition is governed by the parameter $N_{\rm a}r_0$.

On the basis of the above formulas for the braking force acting on a cluster, let us define the cluster mobility in a gas in a weak electric field:

$$K = Z\,\frac{w}{F}\,. \tag{3.5}$$

The force acting on a cluster in an external electric field of a strength E is determined as follows: $F = ZeE$, where Z is the cluster charge expressed in electron charges. This gives the respective relationships for the cluster mobility in the kinetic ($K_{\rm kin}$) and diffusion ($K_{\rm dif}$) regimes:

$$K_{\rm kin} = \frac{3e}{8\sqrt{2\pi mT}N_{\rm a}r_0^2} = \frac{K_0}{n^{2/3}}\,,$$
$$K_0 = \frac{3e}{8\sqrt{2\pi mT}N_{\rm a}r_{\rm W}^2}\,, \quad r_0 \ll \lambda\,, \tag{3.6}$$

$$K_{\rm dif} = \frac{e}{6\pi r_0\eta} = \frac{K_1}{n^{1/3}}\,, \quad K_1 = \frac{e}{6\pi r_{\rm W}\eta}\,, \quad r_0 \gg \lambda\,. \tag{3.7}$$

The cluster mobility in the whole range of parameters, by analogy with formula (3.4) for the force acting on the cluster, takes the form

$$K = K_{\rm kin} + K_{\rm dif}\,. \tag{3.8}$$

Let us determine the cluster mobility in the kinetic regime in an electric field from another standpoint using a small parameter that is the ratio of the atom to cluster masses. In contrast to the above formulas for the cluster mobility, related to a weak electric field strength, employment of this small parameter allows us to consider a wide range of electric field strengths. The peculiarity of motion of a heavy ion in a light gas is the narrow velocity distribution function of ions [80] that is determined either by the thermal velocity of ions or by the mean change in the ion velocity after collision with a gas atom. Since an ion thermal velocity is small compared to a thermal velocity of atoms, and a change in the ion velocity after one collision is small compared with its velocity, the velocity distribution function of ions may be represented in the form $f(\mathbf{v}) = C\delta(\mathbf{v}-\mathbf{w})$, where C is the normalization constant, and $\mathbf{w}$ is the ion drift velocity. Substituting this expression into the kinetic equation for the velocity distribution function of ions, we obtain the relation between the electric field strength E and the ion drift velocity w [80]:

$$\frac{eE}{mN_{\rm a}} = \sqrt{\frac{2T}{\pi m}}\,\frac{\exp\left(-mw^2/2T\right)}{w^3}\int_0^\infty \exp\left(-\frac{mg^2}{2T}\right)$$
$$\times\, g^2\sigma^*(g)\,{\rm d}g\left[\frac{mwg}{T}\cosh\left(\frac{mwg}{T}\right) - \sinh\left(\frac{mwg}{T}\right)\right], \tag{3.9}$$

where m is the gaseous atom mass, $N_{\rm a}$ is the number density of gas atoms, and $\sigma^*(g)$ is the diffusion cross section of atom–cluster scattering which, in accordance with formula (2.4), has the form $\sigma^*(g) = \pi r_0^2$. In the limit of low electric field strengths that corresponds to $mwg \ll T$ in the integrand, the

above relation is transformed to formula (3.1) for the drift velocity of a charged cluster. Formula (3.9) also allows us to find the criterion of validity of formula (3.1) for the cluster drift velocity with respect to the electric field strength. Namely, formula (3.1) holds true if the cluster drift velocity is small compared to the atom thermal velocity (not to the cluster thermal velocity). Next, formula (3.9) in the limit of high electric field strengths ($\sigma^*(g) = \pi r_0^2$) gives

$$w = \sqrt{\frac{eE}{mN_a\sigma^*}}, \quad w \gg \sqrt{\frac{T}{m}}. \tag{3.10}$$

3.2 Relaxation of clusters in a gas flow

On the basis of the above formulas for the braking force acting on a moving cluster in a buffer gas, one can analyze the dynamics of cluster relaxation in a gas flow if the cluster velocity differs from the gas flow velocity. Then, the equation of motion for the cluster relative to the gas flow (or gas in rest) assumes the following form in the diffusion regime of cluster–gas interaction:

$$M\frac{d\mathbf{w}}{dt} = -6\pi\eta r_0\mathbf{w},$$

where M is the cluster mass, and $\mathbf{w}$ is the current cluster velocity. This equation has the following solution

$$\mathbf{w} = \mathbf{v}_0 \exp\left(-\frac{t}{\tau_{rel}}\right),$$

where $\mathbf{v}_0$ is the initial cluster velocity with respect to a gas, and the cluster velocity relaxation time is given by

$$\tau_{rel} = \frac{M}{6\pi r_0\eta} = \tau_0\left(\frac{r_0}{r_W}\right)^2 = \tau_0 n^{2/3}, \quad \tau_0 = \frac{m_a}{6\pi r_W\eta}, \tag{3.11}$$

where m_a is the gaseous atom mass, n is the number of cluster atoms, and η is the gas viscosity. Notably, the reduced relaxation time is $\tau_0 = 4.5\times10^{-11}$ s for large water particles moved in atmospheric air.

Replacing the Stokes force (3.2) in the kinetic regime of cluster–gas interaction by the braking force (3.1), we obtain the expression for the relaxation time:

$$\tau_{rel} = \frac{3M}{8\sqrt{2\pi mT}\,N_a r_0^2} = \frac{n^{1/3}}{k_{rel}N_a}, \quad k_{rel} = \frac{8\sqrt{2\pi mT}\,r_W^2}{3m_a}. \tag{3.12}$$

Here, M is the cluster mass, m_a is the cluster atom mass, m is the gaseous atom mass, and N_a is the number density of gas atoms or molecules. In particular, for large water clusters moving in atmospheric air at the temperature $T = 300$ K, formula (3.12) gives for the relaxation rate constant in the diffusion regime of cluster–gas interaction: $k_{rel} = 2.8\times10^{-11}$ cm^3 s^{-1}, and for large copper clusters moving in argon we have in this case $k_{rel} = 2.3\times10^{-11}$ cm^3 s^{-1}.

According to the above results, a typical time of the cluster velocity relaxation in a gas flow significantly exceeds that for atomic particles because of the large cluster mass. This can lead to violation of the equilibrium between the gas and cluster velocities if the gas velocity varies sharply. This situation takes place if a gas with clusters flows through an orifice from a chamber into a vacuum or a rarefied gas. Then, the gas velocity near the orifice is on the order of the sound speed, and if the radius of the orifice is small compared to that of the chamber, the gas velocity in the chamber is significantly less than the sound speed. In this case, the gas flow velocity varies sharply near the orifice, and the cluster velocity has no time to follow the gas flow velocity; the cluster velocity near the exit orifice may then be small compared with the gas flow velocity. This cluster velocity depends on the chamber profile and is governed by a small parameter τ_{or}/τ_{rel}, where τ_{rel} is the above relaxation time for the cluster velocity, and τ_{or} is a variation time for the gas flow velocity near the orifice. If a gas flows through an orifice, where its velocity is close to the sound speed c_s, the time of variation of the flow velocity is $\tau_{or} = \rho_0/(c_s\tan\alpha)$, where ρ_0 is the orifice radius, and α is the angle between the walls of the conical tube that connects the chamber with the orifice and its axis. Correspondingly, because the cluster drift velocity near the orifice is lower than the gas flow velocity, the cluster concentration increases near the orifice, being inversely proportional to the above small parameter.

On the basis of the above formulas, one can determine the mean free path Λ of clusters in a gas with respect to any variation in its velocity and motion direction. At the beginning, let the cluster velocity with respect to average gas velocity be $\mathbf{v}_0$, so that in the course of relaxation it tends to zero. Based on the above expression for a current cluster velocity $\mathbf{w} = \mathbf{v}_0\exp(-t/\tau_{rel})$, we find the cluster path during relaxation, i.e., the cluster mean free path in a gas, to be $\Lambda = v_0\tau_{rel}$. Taking as the initial cluster velocity its average thermal velocity $v_0 = \bar{v} = \sqrt{8T/\pi M}$, where $M = m_a n$ is the cluster mass, m_a is the cluster atom mass, and n is the number of cluster atoms, we obtain in the kinetic regime of cluster–gas interaction the following expression for the mean free path of the cluster with respect to a change in its motion direction:

$$\Lambda = \bar{v}\tau_{rel} = \frac{3}{4}\sqrt{\frac{m_a}{m}}\,\frac{1}{N_a r_W^2 n^{1/6}}. \tag{3.13}$$

Comparing this quantity with the mean free path of atoms in a buffer gas, $\lambda = 1/N_a\sigma_g$, we find

$$\frac{\Lambda}{\lambda} = \frac{C}{n^{1/6}}, \quad C = \frac{3}{4}\sqrt{\frac{m_a}{m}}\,\frac{\sigma_g}{r_W^2}. \tag{3.14}$$

Table 4 contains the values of the parameter C for some clusters and gases.

3.3 Cluster diffusion in a gas

In determining the cluster diffusion coefficient in a gas, we apply the Einstein relation connecting the cluster mobility in a weak electric field and its diffusion coefficient in a gas:

$$K = \frac{eD}{T}. \tag{3.15}$$

Though this relation has Einstein's name, because he used it in the analysis of the Brownian motion of particles in a gas

Table 4. Values of the parameter C according to formula (3.14) at a temperature of 300 K.

Cluster \ Gas	He	Air	Ar	Xe	CO_2
Na	5.1	5.7	4.6	4.7	8.9
Cu	18	20	16	16	31
Ag	18	20	17	17	32
W	25	28	23	23	44
Au	25	28	23	23	44

Table 5. The reduced diffusion coefficient D_0 for metal clusters in the kinetic regime of atom–cluster collisions in accordance with formula (3.16) [89]. The D_0 values relate to the argon temperature 1000 K, and the normal number density of argon atoms, $N_a = 2.69 \times 10^{19}$ cm^{-3}.

Cluster	D_0, cm^2 s^{-1}	Cluster	D_0, cm^2 s^{-1}
Ti	0.91	Pd	1.01
V	1.05	Ta	0.90
Fe	1.17	W	0.98
Co	1.20	Re	1.01
Ni	1.22	Os	1.05
Zr	0.74	Ir	1.01
Nb	0.90	Pt	0.98
Mo	0.98	Au	0.93
Rh	1.05	U	0.81

[81–83], it had been obtained long before by Nernst [84] and by Townsend and Bailey [85, 86] (see also monographs [87, 88]). Using the Einstein relation (3.15), we obtain on the basis of formulas (3.6) and (3.7) the expressions for the cluster diffusion coefficient in a gas for the kinetic and diffusion regimes of cluster–gas interaction:

$$D_{\rm kin} = \frac{3\sqrt{T}}{8\sqrt{2\pi m}\, N_a r_0^2} = \frac{D_0}{n^{2/3}}\,, \quad D_0 = \frac{3\sqrt{T}}{8\sqrt{2\pi m} N_a r_W^2}\,, \quad \lambda \gg r_0\,;$$

$$D_{\rm dif} = \frac{T}{6\pi r_0 \eta} = \frac{d_0}{n^{1/3}}\,, \quad d_0 = \frac{T}{6\pi r_W \eta}\,, \quad \lambda \ll r_0\,. \qquad (3.16)$$

As is seen, the diffusion coefficient in the kinetic regime is almost independent of the cluster material. Table 5 contains the values of the reduced diffusion coefficient of metal clusters in argon calculated according to formula (3.16) for the kinetic regime of cluster–gas interaction.

One can represent formula (3.16) for the kinetic regime of cluster–gas interaction in the form [90]

$$D = D_* \left(\frac{b}{r_0}\right)^2 .$$

In particular, let us consider diffusion of a large cluster in air for the kinetic regime of cluster–gas interaction, taking $b = 1$ Å. We then obtain for the parameter of this formula: $D_* N_a = 1.2 \times 10^{20}$ cm^{-1} s^{-1}.

One can join formulas (3.16) for the diffusion coefficients in the kinetic and diffusion regimes of cluster–gas interaction, as was done earlier for the cluster mobility. This yields

$$D = D_{\rm kin} + D_{\rm dif}\,,$$

and the last formula may be represented in the form

$$D = \frac{T}{6\pi r_0 \eta}\,(1 + 0.96\,{\rm Kn})\,, \qquad (3.17)$$

which is converted into formula (3.16) in the limit of small and large Knudsen numbers. In particular, for water clusters in air at the temperature 300 K, this formula takes the form

$$D = \frac{k_*}{r_0}\left(1 + \frac{1}{N_a r_0 s_0}\right),$$

where N_a is the number density of air molecules, and the parameters of this formula are: $k_* = 1.2 \times 10^{-11}$ cm^3 s^{-1}, and $s_0 = 4.3 \times 10^{-19}$ cm^2.

Since the pair interaction potential of atoms in the range of their repulsion varies sharply with variations of the distance between atoms, the scattering of two colliding gas atoms is described by the hard sphere model and has the same character as atom–cluster scattering. Hence, the ratio of the diffusion coefficient of clusters in a gas, $D_{\rm kin}$, in the kinetic regime of cluster–gas interaction and the self-diffusion coefficient D_a for gas atoms may be represented in the form

$$\frac{D_{\rm kin}}{D_a} = \left(\frac{\rho_0}{r_0}\right)^2 ,$$

where ρ_0 is the effective radius of atomic interaction that determines the gas-kinetic cross section $\sigma_g = \pi\rho_0^2$ and depends weakly on the gas temperature. Specifically, for atmospheric air at a temperature of 300 K, the parameters of the above formula are [90]: $\rho_0 = 3.6$ Å, $D_a N_a = 4.8 \times 10^{18}$ cm^{-1} s^{-1}, $DN_a r_0^2 = 4.4 \times 10^3$ cm s^{-1}, and N_a is the number density of air molecules.

In considering the dynamics of cluster motion in a gas in the diffusion regime of cluster–gas interaction, we assumed the Reynolds number to be small. Let us ascertain the validity of this assumption for cluster free fall in atmospheric air. The cluster free fall velocity **w** then follows from the equality between the gravitational force and braking force, and the force balance gives

$$\frac{4\pi}{3}\,\rho\,\mathbf{g}\,r_0^3 = 6\pi\eta r_0 \mathbf{w}\,,$$

where ρ is the density of the cluster material, and g is the free fall acceleration. Hence it follows that the velocity of falling cluster is defined as

$$w = \frac{2\rho g r_0^2}{9\eta}\,. \qquad (3.18)$$

Let us determine the Reynolds number in accordance with the formula

$${\rm Re} = \frac{w r_0}{\nu}\,, \qquad (3.19)$$

where $\nu = \eta/\rho_g$ is the gas kinematic viscosity, so that η and ρ_g are the viscosity and density of the gas, respectively. From this, we find the condition for the cluster radius where the Reynolds number is small (Re $\ll$ 1):

$$r_0 \ll \frac{\eta^{2/3}}{(\rho\rho_g g)^{1/3}}\,. \qquad (3.20)$$

In particular, this criterion gives $r_0 \ll 30$ μm for water drops moving in atmospheric air. It should be emphasized that this drop size is the boundary between the kinetic and diffusion regimes of cluster–gas interaction at the number density of air molecules $N_a = 9 \times 10^{16}$ cm^{-3} or the air pressure $p = 2.5$ Torr at a temperature of 300 K.

Thus, the above analysis exhibits a smooth transition between the kinetic and diffusion (or hydrodynamic) regimes of cluster–gas interaction if the cluster radius and the mean free path of gas atoms or molecules become comparable.

4. Collisions of atoms and molecules with clusters and small particles in a buffer gas

4.1 Equilibrium of a metal cluster with a parent vapor in a buffer gas

There is a group of processes resulting from collisions of admixture atoms located in a buffer gas with the cluster

surface. The growth of clusters as a result of the attachment of admixture atoms of the same sort, quenching of metastable atoms in collisions with the cluster surface, recombination of electrons and ions at the cluster surface, and cluster combustion in an oxygen-containing mixture relate to this group of processes. We consider first the simplest among these processes, which consists in atom attachment to the cluster surface. This process takes place if metal atoms are an admixture to a buffer gas where metal clusters of the same sort are located. At a low temperature, which is assumed to be identical for the buffer gas, metal vapor, and metal clusters, one can neglect atom evaporation from the cluster surface, and clusters grow as a result of the attachment of metal atoms. Below, we will determine the rate constant of this process.

In the limit of a high concentration of metal atoms, each of the metal atoms nearest to the cluster can reach the cluster surface without collisions with buffer gas atoms. For simplicity, we will assume that each contact of a free metal atom with the cluster surface leads to its attachment. The rate constant of this process is given by formula (2.5), and the kinetics of cluster growth is described by the following balance equation

$$\frac{\mathrm{d}n}{\mathrm{d}t} = k_0 n^{2/3} N_\mathrm{m}\,, \quad k_0 = \sqrt{\frac{8T\pi}{m_\mathrm{a}}}\, r_\mathrm{W}^2\,. \tag{4.1}$$

Here, n is the number of cluster atoms, N_m is the number density of free metal atoms, T is the gas temperature expressed in energy units, m_a is the metal atom mass, and r_W is the Wigner–Seitz radius. The solution of this equation for a current number n of cluster atoms leads to the following connection between n and time t of its growth, under the assumption that the number density N_m of free metal atoms is kept constant in the course of cluster growth:

$$n = \left(\frac{k_0 N_\mathrm{m} t}{3}\right)^3. \tag{4.2}$$

In the case of the diffusion regime of cluster growth, the rate J of cluster growth, i.e., the number of attaching atoms per unit time, is given by the Smoluchowski formula (2.8).

The metal atom diffusion coefficient in a buffer gas in the first Chapman–Enskog approximation [75, 76] is defined as

$$D_\mathrm{m} = \frac{3\sqrt{\pi T}\lambda_\mathrm{m}}{8\sqrt{2\mu}} = \frac{3\sqrt{\pi T}}{8\sqrt{2\mu}\, N_\mathrm{a}\sigma_\mathrm{m}}\,, \tag{4.3}$$

where λ_m is the mean free path of a metal atom in the buffer gas, $\mu = mm_\mathrm{a}/(m+m_\mathrm{a})$ is the reduced mass of a metal atom and buffer gas atom, and σ_m is the diffusion cross section of collision between a metal atom and a buffer gas atom that is averaged over atomic velocities. On the basis of the Smoluchowski formula (2.8), we have the following balance equation for cluster growth in the diffusion regime:

$$\frac{\mathrm{d}n}{\mathrm{d}t} = 4\pi D_\mathrm{m} r_0 N_\mathrm{m} = 4\pi D_\mathrm{m} r_\mathrm{W} N_\mathrm{m}\, n^{1/3}\,. \tag{4.4}$$

Let us compare the rates of cluster growth as a result of atom attachment in the kinetic and diffusion regimes. On the basis of formulas (4.1) and (4.4), we have the ratio of these growth rates:

$$\frac{J_\mathrm{dif}}{J_\mathrm{kin}} = \frac{3\pi\sqrt{2}}{8}\sqrt{\frac{m_\mathrm{a}+m}{m_\mathrm{a}}}\,\frac{\lambda_\mathrm{m}}{r_0} = 1.67\sqrt{\frac{m_\mathrm{a}+m}{m_\mathrm{a}}}\,\frac{\lambda_\mathrm{m}}{r_0}\,. \tag{4.5}$$

As is seen, the growth rates are close if the mean free path λ_m for a metal atom in a buffer gas is comparable to the cluster radius r_0. There is an analogy here with the transport parameters of clusters in a buffer gas, which are determined by formulas (3.4) and (3.17). But in contrast to cluster transport phenomena, nearby values of the cluster growth rates do not mean the transition from one interaction mechanism to another. The criterion of validity of these regimes is based on a comparison between the mean free path λ_m of a metal atom in a buffer gas with a typical distance from a cluster to a nearest metal atom, $N_\mathrm{m}^{-1/3}$, so that in the limiting case where

$$N_\mathrm{m}^{1/3}\lambda_\mathrm{m} \ll 1\,, \tag{4.6}$$

the diffusion regime of atom attachment to the cluster surface is realized, and for the opposite criterion with respect to criterion (4.6) the kinetic regime of atom attachment to the cluster surface in a buffer gas takes place.

At a high temperature in the system under consideration consisting of a buffer gas, gas of metal clusters, and atomic metal vapor, atomic evaporation from the cluster surface is of importance. If the rate constants of cluster evaporation and atom attachment are equalized, equilibrium is established between the gas of clusters and metal vapor. We first determine the equilibrium number density of metal atoms located near the cluster in the kinetic regime of interaction between the clusters and buffer gas, if free metal atoms reach the cluster surface without collisions with buffer gas atoms. For a cluster of infinite size with an almost flat surface, this equilibrium takes place at the number density $N_\mathrm{sat}(T)$ of atoms, which corresponds to the saturated vapor pressure at a given temperature:

$$N_\mathrm{m} = N_\mathrm{sat}(T)\,. \tag{4.7}$$

The temperature dependence for the number density of atoms at saturation has the form

$$N_\mathrm{sat}(T) \sim \exp\left(-\frac{\varepsilon_0}{T}\right),$$

where ε_0 is the binding energy of a metal atom with the flat surface. When passing from the flat metal surface to a spherical cluster, we assume this dependence to be basic, and then the equilibrium number density of metal atoms with respect to clusters consisting of n atoms is found to be

$$N_\mathrm{m} = N_\mathrm{sat}(T)\exp\left(\frac{\varepsilon_0}{T} - \frac{\varepsilon_n}{T}\right), \tag{4.8}$$

where ε_n is the atom binding energy in the cluster consisting of n atoms. Let us represent the total binding energy of cluster atoms as a sum of the volume and surface parts [91]:

$$E_n = \varepsilon_0 n - An^{2/3}\,,$$

where ε_0 is the binding energy per atom for a bulk system of bound atoms, and A is the specific surface cluster energy. From this follows the expression for the binding energy of a surface cluster atom:

$$\varepsilon_n = \frac{\mathrm{d}E_n}{\mathrm{d}n} = \varepsilon_0 - \frac{2A}{3n^{1/3}}\,, \tag{4.9}$$

and formula (4.8) for the equilibrium number density of free metal atoms takes the form

$$N_{\rm m} = N_{\rm sat}(T)\,\exp\left(\frac{2A}{3n^{1/3}}\right). \tag{4.10}$$

Note that the above monotonic dependence of the atomic binding energy on the number n of cluster atoms holds true for liquid clusters, while for solid clusters dependence (4.9) is valid on average.

Let us determine the rate of atom evaporation from the cluster surface that follows from equality of the rates of atom attachment and atom evaporation under equilibrium conditions. Using formula (4.10) for the equilibrium number density of free metal atoms, we obtain the cluster evaporation rate in the kinetic regime of cluster interaction with a buffer gas atom:

$$\nu_{\rm kin} = k_0 N_{\rm sat}(T)\exp\left(\frac{2A}{3n^{1/3}}\right), \tag{4.11}$$

and the corresponding formula follows for the diffusion regime of cluster interaction with a buffer gas:

$$\nu_{\rm dif} = 4\pi D_{\rm m} r_0 N_{\rm sat}(T)\exp\left(\frac{2A}{3n^{1/3}}\right). \tag{4.12}$$

The rate of atom evaporation from the cluster surface, together with the rate of attachment of free atoms to the cluster surface, determines cluster equilibrium with a surrounding dense vapor. It would seem that this evaporation rate is only determined by the cluster properties and does not depend on the character of motion of free cluster atoms near the cluster. But taking into account that the evaporation rate includes only such evaporated atoms which move far from the cluster surface (and in this manner excluding those atoms which return to the cluster surface), we obtain different expressions for the evaporation rates in the kinetic and diffusion regimes of cluster interaction with a buffer gas.

4.2 Quenching of metastable atoms by clusters and cluster combustion

Metastable atoms are destroyed effectively upon contact with the cluster surface. This process for metal clusters is similar to that for collision of a metastable atom with a metal surface, where the conduction electrons interact with a valence electron of the metastable atom and transfer this atom to the ground state. For a dielectric cluster, this process is analogous to collision of a metastable atom with another atom or molecule, but a large number of channels are possible in the cluster for quenching the metastable state. Therefore, the probability of quenching the metastable atomic state as a result of contact with the cluster surface (sticking probability) is on the order of unity. Assuming for simplicity this probability to be unity, we use formulas (4.1) and (4.3) for the rate constant of atom–cluster collisions with their contact. Hence, the rate constant of quenching of the metastable atomic state in atom–cluster collisions, taking into account the above assumption, has the following form for the kinetic and diffusion regimes of atom–cluster interaction:

$$k_{\rm kin} = k_0 n^{2/3}, \quad k_{\rm dif} = 4\pi D_{\rm m} r_0\,, \tag{4.13}$$

where $D_{\rm m}$ is the diffusion coefficient of metastable atoms in a buffer gas. Because the concentration of metastable atoms in a buffer gas is small, quenching of metastable atoms in a buffer gas with clusters proceeds in the diffusion regime of cluster–gas interaction in accordance with criterion (4.6).

Combustion of clusters or small particles in an oxygen-containing gaseous mixture proceeds as the above processes do as a result of contact between the oxygen molecule and the cluster surface, and we will consider this process within the framework of a simplified scheme. Indeed, the chemical process of oxidation of a material and formation of oxides proceeds in several stages, and part of them takes place on the cluster surface, whereas the other processes involving forming radicals proceed in a gas phase or in a new phase formed by radicals. Considering the total process to be on the cluster surface, we hence assume the transport of oxidant (oxygen molecules) to an oxidable object (cluster) as the slowest process in the chain of combustion processes. This assumption allows us to determine the lower boundary of the rate for the total process of material oxidation. Below, we restrict ourselves to the diffusion regime of cluster oxidation as the most probable regime for this process. Thus, when transferring the above model of collisions of an admixture atom and cluster to the process of cluster oxidation in an oxygen-containing buffer gas, we employ the assumption that the contact of the oxygen molecule with the cluster provides the total use of this molecule to obtain the final product of the chemical reaction. Correspondingly, the rate constant of the total process is determined by the Smoluchowski formula (2.8), which now gives for the rate constant of the chemical reaction:

$$k_{\rm chem} = 4\pi D_{\rm ox} r_0\,, \tag{4.14}$$

where $D_{\rm ox}$ is the diffusion coefficient of oxygen molecules in a buffer gas.

Let us analyze one more aspect of this process. Both the quenching of a metastable atom in collision with a cluster and cluster combustion in an oxygen-containing gaseous mixture are accompanied by significant energy release, which leads to an increase in the cluster temperature, and this, in turn, can accelerate the process substantially. The released energy heats not only the cluster, but also a surrounding gas, and creates heat fluxes from the cluster. Because of the cluster smallness, convective fluxes are absent in heat transport, and cooling of the cluster and gas near it is governed by the thermal conductivity of a buffer gas. Let us analyze the heat balance equation in this case by introducing the energy $\Delta\varepsilon$ released per metastable atom or per oxygen molecule in cluster combustion. The flux $\mathbf{j}$ of active particles, i.e., metastable atoms or oxygen molecules, takes the following form $\mathbf{j} = -DN_{\rm a}\nabla c$, where D is the diffusion coefficient of active particles in a buffer gas, $N_{\rm a}$ is the number density of buffer gas atoms, and c is the concentration of active particles. The heat flux $\mathbf{q}$ is expressed in this case as

$$\mathbf{q} = -\kappa\nabla T = \Delta\varepsilon\mathbf{j} = -\Delta\varepsilon D N_{\rm a}\nabla c\,, \tag{4.15}$$

where κ is the thermal conductivity coefficient of a buffer gas. From Eqn (4.15) we obtain the equation relating the current concentration of active particles in a buffer gas to the buffer gas temperature:

$$\frac{{\rm d}c}{{\rm d}T} = \frac{\kappa}{\Delta\varepsilon D}\,. \tag{4.16}$$

Table 6. The logarithmic derivatives over the temperature for the self-diffusion coefficient D of atoms in inert gases, the thermal conductivity coefficient κ, and the viscosity coefficient η for inert gases in the temperature range 300–1000 K in accordance with the data of handbooks [92, 93].

Gas	He	Ne	Ar	Kr	Xe
$-\mathrm{d}\ln D/\mathrm{d}\ln T$	1.73	1.69	1.70	1.78	1.76
$-\mathrm{d}\ln \kappa/\mathrm{d}\ln T$	0.71	0.70	0.75	0.80	0.86
$-\mathrm{d}\ln \eta/\mathrm{d}\ln T$	0.68	0.66	0.74	0.77	0.85

Equation (4.16) gives the temperature difference T_{cl} between the cluster surface and a buffer gas far from the cluster. This temperature difference is created by the heat balance on the cluster surface, where active particles go to the cluster surface as a result of their diffusion in a buffer gas, while heat release is determined by the thermal conductivity of a buffer gas, and is given by

$$T_{\mathrm{cl}} = \frac{\Delta\varepsilon D}{\kappa}\, c_0\,, \tag{4.17}$$

where c_0 is the concentration of metastable atoms or oxygen molecules in a buffer gas far from the cluster. Relation (4.17) relies on the assumption that the kinetic coefficients D and κ are independent of the temperature.

As follows from equation (4.16), the concentration of active particles that is zero on the cluster surface increases upon removal from the cluster and tends to the equilibrium value c_0. For determination of the spatial distribution of the concentration of active particles near the cluster surface, it is necessary to take into account the temperature dependence for transport coefficients, such as the diffusion coefficient D, the thermal conductivity coefficient κ, and the viscosity coefficient η, and we use such a dependence in the temperature range $T = 300-1000$ K. The values of appropriate parameters are given in Table 6 and are based on the data from handbooks [92, 93].

In conclusion of this section, we consider the criteria of validity of the kinetic and diffusion regimes of collision of given atomic particles with a cluster. According to formula (4.13), the kinetic regime for atom–cluster collisions requires the criterion

$$r_0 \ll \frac{4\pi D r_{\mathrm{W}}^2}{k_0}\,, \tag{4.18}$$

where D is the diffusion coefficient of atomic particles in a buffer gas. Since the diffusion coefficient is inversely proportional to the number density of buffer gas atoms, a decrease in the gas pressure leads to an increase in the maximum cluster size for the kinetic regime of atom–cluster interactions. As an example we consider the attachment of silver atoms to a silver cluster in the course of cluster growth in the magnetron discharge in argon [11] at an argon pressure of 0.1 Torr and a temperature of 1000 K. In this case, the parameters of formula (4.18) are the following: $r_{\mathrm{W}} = 1.66$ Å according to the data of Table 1, $k_0 = 3.8\times10^{-11}$ cm^3 s^{-1} according to the data of Table 3, and $D = 800$ cm^2 s^{-1} [94], so that the kinetic regime of atom–cluster interactions is realized for $r_0 \ll 1$ μm. Thus, the kinetic regime of atom–cluster interactions for the growth of metal clusters takes place in a magnetron discharge where the size of the clusters formed is $r_0 \ll 100$ nm [94].

5. Kinetics of charging for clusters and small particles in an ionized gas

5.1 Self-consistent field of cluster and ionized gas in the kinetic regime involving free ions

Charged microparticles located in weakly ionized gases are one of the basic components of the dusty plasma [95–101]. The charged particle field influences the distribution of ions and electrons near it, and this redistribution leads to creation of a self-consistent field which is determined by both the charged particle field and ions and electrons near the particle. Moreover, the particle charge depends on the currents of electrons and ions to the particle surface. Thus, both the particle charging and the particle charge screening result from the action of the self-consistent particle field. Determination of this self-consistent field of the particle and ionized gas is our first task. This allows us to determine the radius of action of the particle field in an ionized gas, which is an important parameter in studying the interaction of a particle with a surrounding ionized gas.

Colliding with the particle surface, electrons and ions attach to it, and subsequent recombination of electrons and ions proceeds on the particle surface. Absorption of electrons and ions by the particle influences the screening of the particle field by electrons and ions in an ionized gas. For this reason, the screening of the particle field differs from the Debye screening [102, 103], and the latter phenomenon occurs only far from the particle. Our goal is to ascertain the character of the creation of the self-consistent field for the particle and surrounding ionized gas, and the screening of the particle field separately for the kinetic and diffusion regimes of particle–gas interactions.

The character of recombination of electrons and ions on the surface of a cluster or small particle in an ionized gas differs from that of cluster collisions with neutral atomic particles in a buffer gas. Below, we will call the particles as clusters because of the identical character of processes within the framework of macroscopic models used for them. The attachment of electrons and ions to a cluster leads to their charging and creates the self-consistent field that, in turn, influences the distribution of electrons and ions near the charged cluster. A charged cluster then creates an electric field around itself that prevents electrons from approaching the cluster and equalizes in this manner the electron and ion currents to the cluster surface. As a result, a stationary field and stationary distributions of electrons and ions are produced in the region of action of the cluster field.

A cluster is charged negatively because the electron mobility is higher than the ion mobility, and it is surrounded by an ion cloud, so that the radius l of action of the cluster field is determined by ions located in its field and exceeds remarkably the cluster radius r_0. The radius of action of the cluster field may be derived from the relation

$$U(l) \sim T_{\mathrm{i}}\,, \tag{5.1}$$

where $U(R)$ is the potential energy for an electron located in the field of the cluster and a surrounding ionized gas at a distance R from the cluster, and T_{i} is the ion temperature expressed in energy units. The kinetic regime of interaction of a charged cluster with surrounding electrons and ions corresponds to the criterion

$$\lambda_{\mathrm{i}} \gg l\,, \tag{5.2}$$

where λ_i is the mean free path of ions in a buffer gas. If this criterion holds true, an ion passes through a region of its strong interaction with a self-consistent field of a cluster and ionized gas without collisions with buffer gas atoms, thus corresponding to the kinetic regime of interaction between the cluster and a buffer gas. We will determine below the cluster charge and also the electron and ion distributions near the cluster. For simplicity, we first assume that all ions located far from the cluster possess energy ε and number density N_0 that coincides with the number density of electrons because of the plasma quasineutrality. Then, we have for ions in the region of action of the cluster field the following relation [104]

$$\mathrm{d}t = \frac{\mathrm{d}R}{v_R} = \frac{\mathrm{d}R}{v\sqrt{1-\rho^2/R^2 - U(R)/\varepsilon}}\,,$$

where $\mathrm{d}t$ is the time interval during which the ion resides in a distance range between R and $R+\mathrm{d}R$, $v_R(R)$ is the normal component of the ion velocity towards the cluster at a distance R from it, v is the ion velocity far from the cluster, $\varepsilon = m_\mathrm{i}v^2/2$ is the ion kinetic energy far from the cluster, so that m_i is the ion mass, and ρ is the impact parameter of ion motion with respect to the cluster center.

Transferring on the basis of the ergodic theorem [105–107] from dynamics of an individual particle to statistical mechanics, which concerns the distribution of an ensemble of particles in a space [103, 108], we find the probability $\mathrm{d}P_\mathrm{i}$ of ion location in a given space region being proportional to the time interval that an individual particle resides in this space region: $\mathrm{d}P_\mathrm{i} \sim \mathrm{d}t$, and the number density of ions being proportional to this probability: $N_\mathrm{i}(R) \sim \mathrm{d}P_\mathrm{i}$. Therefore, we have the following relation for the ion number density in a given region in space:

$$N_\mathrm{i} \sim \frac{\int \rho\,\mathrm{d}\rho\,\mathrm{d}P_\mathrm{i}}{4\pi R^2\,\mathrm{d}R}\,.$$

Normalizing this relation and transferring to the limit where interaction is absent, so that the ion number density is $N_\mathrm{i} = N_0$, we obtain

$$N_\mathrm{i}(R) = N_0\int_0^{\rho(R)} \frac{\rho\,\mathrm{d}\rho}{R^2\sqrt{1-\rho^2/R^2 - U(R)/\varepsilon}}\,, \qquad (5.3)$$

where, in the case of free ion motion, $U(R) = 0$, the impact parameter of ion–cluster collision with a distance of closest approach R is given by the relation $\rho(R) = R$.

Taking into account the influence of the self-consistent cluster and plasma fields on ion motion, let us divide ion trajectories into two groups, and the ion is captured by a cluster for trajectories of the first group, which takes place for impact parameters of collision $\rho \leqslant \rho_\mathrm{c}$, where ρ_c is the impact parameter of collision above which the ion capture is impossible. The impact parameter of the ion contact with a cluster of a radius r_0 is given by [104]

$$\rho_\mathrm{c}^2 = r_0^2\left[1 - \frac{U(r_0)}{\varepsilon}\right].$$

For trajectories of the second group, where ions go to infinity after collision with the cluster, the total number density of ions in the cluster field takes the form [109]

$$N_\mathrm{i}(R) = \frac{N_0}{2}\left[\sqrt{1-\frac{U(R)}{\varepsilon}} + \sqrt{1-\frac{\rho_\mathrm{c}^2}{R^2} - \frac{U(R)}{\varepsilon}}\,\right]. \qquad (5.4)$$

Averaging the ion number density over the Maxwell distribution of ions far from the cluster, which has the form

$$f(\varepsilon) = N_0\,\frac{2\varepsilon^{1/2}}{\sqrt{\pi}\,T_\mathrm{i}^{3/2}}\exp\left(-\frac{\varepsilon}{T_\mathrm{i}}\right),$$

we obtain the number density of ions in the self-consistent field of the cluster and ionized gas [109]:

$$N_\mathrm{i}(R) \approx N_0\left[\sqrt{\frac{|U(R)|}{\pi T_\mathrm{i}}} + \sqrt{\frac{|U(R)| - |U(r_0)|\,r_0^2/R^2}{\pi T_\mathrm{i}}}\,\right]. \qquad (5.5)$$

Since the cluster possesses a negative charge Z and near the cluster $|Z|e^2/r_0 \gg T_\mathrm{i}$, we arrive at the following relation for the ion number density near the cluster surface:

$$N_\mathrm{i}(R) = N_0\sqrt{\frac{|Z|\,e^2}{r_0 T_\mathrm{i}}}, \quad R - r_0 \ll r_0\,,$$

i.e., the number density of ions near the cluster surface exceeds significantly the electron number density and the ion number density far from the cluster. Based on this inference, we will find the self-consistent field potential if it is determined by free ions and the radius of action of the self-consistent field is large: $l \gg r_0$. Then, the number density of ions in the region of action of the self-consistent field is given by the first term in formula (5.5). Let us introduce a current charge $z(R)$ that is equal to the sum of the cluster charge and ion charges inside a sphere of a radius R. In the region of a strong screening of the cluster field by ions, this charge, according to the Gauss theorem [110, 111], satisfies the equation

$$\frac{\mathrm{d}z}{\mathrm{d}R} = -4\pi R^2 N_0\sqrt{\frac{|U(R)|}{T_\mathrm{i}}},$$

with $z(r_0) = |Z|$. Hence, the self-consistent field potential is given by

$$U(R) = \int_R^\infty E(R)\,\mathrm{d}R \approx \frac{z(R)\,e^2}{R}\,.$$

The latter simplification leads to an error, whose magnitude depends on distance R from the cluster center; the corresponding dependence is demonstrated in Fig. 3. Under this simplification, we have the following equation for a current charge $z(R)$ located inside a sphere of a radius R:

$$\frac{\mathrm{d}z}{\mathrm{d}R} = -4\pi R^2 N_0\sqrt{\frac{4ze^2}{\pi T_\mathrm{i} R}},$$

and its solution has the form

$$z = |Z|\left[1 - \left(\frac{R}{l}\right)^{5/2}\right]^2,$$
$$l = \frac{0.66}{N_0^{2/5}}\left(\frac{|Z|\,T_\mathrm{i}}{e^2}\right)^{1/5} = \frac{0.66|Z|^{2/5}}{N_0^{2/5}R_0^{1/5}}\,, \qquad (5.6)$$

where the parameter R_0 is equal to $|Z|e^2/T_\mathrm{i}$, and $R_0 \gg r_0$.

It should be noted that the above consideration relates to a range of distances from a cluster, where the ion–cluster interaction potential significantly exceeds an ion thermal energy. At the boundary of action of the self-consistent cluster field, where the interaction potential is comparable to a thermal energy of ions, the screening is of the Debye

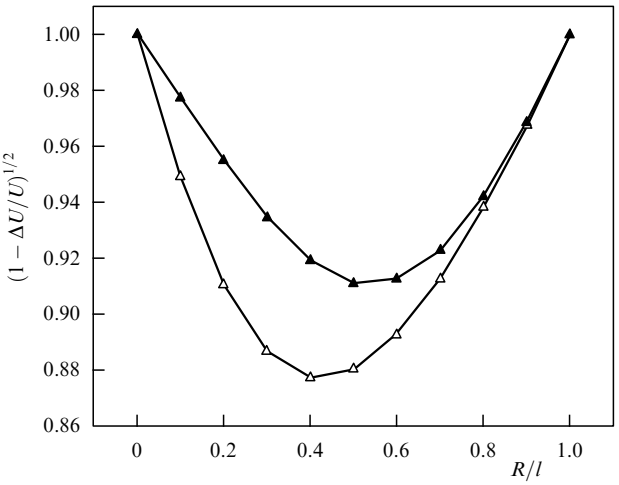

Figure 3. Correction to the potential of ion interaction with a self-consistent field of charged particles located in an ionized gas leads to replacing the self-consistent ion–particle interaction potential $U(R) = z(R)e^2/R$ by the quantity $U(R) - \Delta U = \int_R^\infty ze^2\,\mathrm{d}R/R^2$. Dark triangles describe the case where the screening of the cluster field is determined by free ions, and white triangles relate to the screening of the cluster field by trapped ions.

character. Correspondingly, the kinetic regime of ion interaction with the self-consistent cluster field requires the validity of the criterion

$$N_\mathrm{a} l\sigma^* \ll 1\,,$$

where σ^* is the diffusion cross section for ion–atom scattering, which is assumed to be independent of the collision velocity. In the case of ion scattering in the parent atomic gas at not low collision energies, this scattering is determined by the resonant charge exchange process, so that the cross section of such a process exceeds remarkably that of ion–atom elastic scattering. An ion and atom then move along straightforward trajectories in the course of resonant charge exchange, and the diffusion cross section of ion–atom scattering is $\sigma^* = 2\sigma_\mathrm{res}$ [112], where σ_res is the cross section of the resonant charge exchange. Correspondingly, the criterion for the kinetic regime of screening of the self-consistent cluster field takes the form

$$2N_\mathrm{a} l\sigma_\mathrm{res} \ll 1\,. \tag{5.7}$$

In particular, for argon as a buffer gas, an argon atomic ion as the basic ion sort under the conditions considered, and the ion–atom collision energy of 0.01 eV, we have $\sigma_\mathrm{res} = 83$ Å^2 for the cross section of resonant charge exchange [59]. Here, the kinetic regime is realized at the argon pressure $p \ll 0.1$ Torr for a particle radius of 1 μm and for an ion temperature on the order of room temperature.

To determine the cluster charge in the kinetic regime as a result of attachment of electrons and ions to its surface, we will take into account that the fluxes of electrons and ions towards the cluster are generated outside the region of action of the self-consistent cluster field, and therefore these fluxes are similar to those in the absence of screening of the cluster field. Hence, assuming that each contact of electrons and ions with the cluster surface leads to their attachment to the cluster, we find the rate of ion attachment to the cluster [104]:

$$J_\mathrm{i} = N_\mathrm{i}\sqrt{\frac{8T_\mathrm{i}}{\pi m_\mathrm{i}}}\left(1 + \frac{|Z|\,e^2}{r_0 T_\mathrm{i}}\right)\pi r_0^2\,, \tag{5.8}$$

where N_i is the number density of ions far from the cluster, and T_i is the ion temperature. In the same manner, we obtain the rate of electron attachment to a negative charged cluster in the form

$$J_\mathrm{e} = N_\mathrm{e}\sqrt{\frac{8T_\mathrm{e}}{\pi m_\mathrm{e}}}\pi r_0^2 \exp\left(-\frac{|Z|e^2}{r_0 T_\mathrm{e}}\right), \tag{5.9}$$

where, as before, we employed the cross section for the collision of two charged particles [104], N_e is the electron number density far from the cluster, and T_e is the electron temperature. Equalizing currents of electrons and ions on the cluster surface and assuming the plasma far from the cluster to be quasineutral, $N_\mathrm{i} = N_\mathrm{e} = N_0$, we obtain the following equation for the reduced cluster charge $x = |Z|e^2/(r_0 T_\mathrm{e})$:

$$x = \frac{1}{2}\ln\frac{T_\mathrm{e} m_\mathrm{i}}{T_\mathrm{i} m_\mathrm{e}} - \ln\left(1 + x\,\frac{T_\mathrm{e}}{T_\mathrm{i}}\right). \tag{5.10}$$

Under the usual conditions of $xT_\mathrm{e} \gg T_\mathrm{i}$, this leads to the following reduced cluster charge [113]:

$$x = \frac{1}{2}\ln\frac{T_\mathrm{i} m_\mathrm{i}}{x^2 T_\mathrm{e} m_\mathrm{e}}\,. \tag{5.11}$$

In particular, for the argon gas-discharge plasma being exemplified with parameters $T_\mathrm{e} = 1$ eV and $T_\mathrm{i} = 400$ K, we have $x = 2.86$ or $|Z|/r_0 = 2.0$ nm^{-1}. Note that this consideration holds true at a large cluster charge $|Z| \gg 1$, so that the attachment of an individual electron or ion to a cluster does not change its field. For the above parameters of an argon gas discharge plasma, this corresponds to the criterion $r_0 \gg 0.5$ nm.

Another important parameter of the cluster along with its charge is the radius l of action of the self-consistent cluster field that is determined by formula (5.6). In particular, for the example of an argon plasma being considered with parameters $T_\mathrm{e} = 1$ eV, $T_\mathrm{i} = 400$ K, and the cluster radius $r_0 = 1$ μm, we have $|Z| = 2000$, and for the respective number densities of electrons and ions far from the cluster, $N_0 = 10^9$ cm^{-3} and $N_0 = 10^{10}$ cm^{-3}, we find, according to formula (5.6), $l = 90$ μm and $l = 36$ μm, respectively, which exceeds significantly the cluster radius.

5.2 Self-consistent field of cluster and ionized gas in the kinetic regime involving trapped ions

Along with free ions, trapped ions, i.e., those captured in closed orbits, may be of importance in screening a charged particle [114]. Though the probability of ion capture in closed orbits resulting from resonant charge exchange between an atom and ion in the range of ion strong interaction with a charged cluster is small, the long lifetime of this ion in the closed orbit compensates for this smallness, so that just trapped ions can determine the cluster screening in an ionized gas at low number densities of plasma electrons and ions. The trajectories of trapped ions are different for ion motion in the pure Coulomb field and in the shielded Coulomb field of a charged center [104, 115], as is demonstrated in Figs 4 and 5.

The role of trapped ions in screening the cluster charge was studied widely, in particular, in papers [96, 116–124]. We present a simple and practical version [109] of this phenomenon, taking into account that the cross section σ_res of resonant charge exchange in ion–atom collisions is independent of the collision velocity and exceeds remarkably the cross

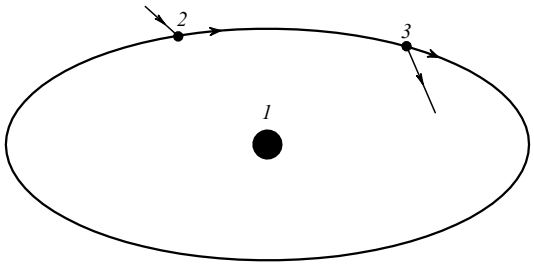

Figure 4. Trajectory of ion motion if the ion is captured in a closed orbit in the electric field of the Coulomb center.

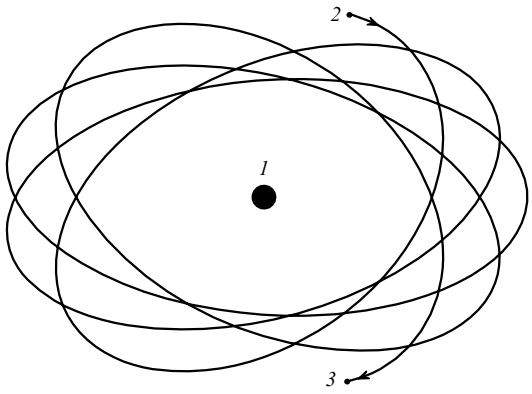

Figure 5. Trajectory of ion motion if the ion is captured in a closed orbit in the screened Coulomb field of a charged center.

section of elastic ion–atom scattering in thermal collisions, so that the colliding ion and atom move along straightforward trajectories (the relay character of charge transfer) [125, 126]. This circumstance restricts the parameters of ion capture in a finite orbit, as shown in Fig. 6. In accordance with the character of ion trajectories, we determine the screening parameters in two limiting cases where they are determined either by free or trapped ions. The closeness of the results for these limiting cases at their border justifies this simplified algorithm of calculations.

In considering ion capture in the cluster field, we apply the criterion

$$R_0 = \frac{|Z|e^2}{T_i} \gg r_0 \,. \tag{5.12}$$

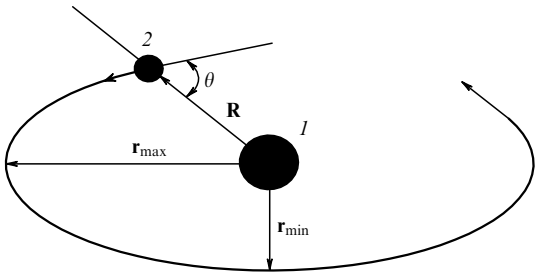

Figure 6. Parameters of a trapped ion formed as a result of resonant charge exchange in the region of strong interaction between a forming ion and cluster: r_{min} is the minimum distance of the ion trajectory from the cluster, r_{max} is the maximum distance from the cluster for a trapped ion, **R** is a point where the resonant charge exchange event has proceeded, and θ is the angle between the ion velocity vector after resonant charge exchange and vector **R** that joins the ion with the cluster center.

A trapped ion may become free if it is located near the boundary of action of the self-consistent cluster field, $R \approx l$, while ions move along closed trajectories if they are captured at a distance $R > \sqrt{r_0 R_0}$ from the cluster center. Therefore, trapped ions may influence the screening of the cluster field if the condition

$$l > \sqrt{r_0 R_0} \tag{5.13}$$

is satisfied. In this case, the subsequent charge transfer process for a trapped ion leads to its transition to closer finite orbits. If the distance between the cluster and ion becomes less than $\sqrt{r_0 R_0}$, the next resonant charge exchange leads to ion falling on the cluster. Therefore, if criterion (5.13) holds true, kinetics of a trapped ion consist of a series of subsequent transitions to orbits, each of them being closer to the cluster than the previous one, and finally the ion will fall on the cluster surface. Since many events of resonance charge exchange between the ion and buffer gas atoms are required for ion capture by the cluster surface, the number density of trapped ions in closed orbits may be large, exceeding the number density of free ions in the limit of a low plasma density. Therefore, the cluster field screening is determined in this limiting case by trapped ions.

In analyzing the kinetics of trapped ions, we rely on the character of the resonant charge exchange process at low collision velocities compared to a typical velocity of the bound atomic electron. Charge exchange then proceeds in accordance with the Sena effect, where an ion and atom move along straightforward trajectories, but a former atom is converted into an ion [125, 127]. An ion acquires the atomic energy ε and the direction of motion of the former atom; in addition, from the conservation laws for energy and momentum [104] it follows that ion capture in a finite orbit that does not touch the cluster surface (i.e., the distance of ion–cluster closest approach r_{min} exceeds the cluster radius r_0) is determined by the relation [109]

$$\frac{R^2}{r_0^2} \leqslant 1 + \frac{U(R) - U(r_0)}{\varepsilon} \,. \tag{5.14}$$

Here, R is the ion–cluster distance at the capture point, ε is the initial energy of a formed ion, and $U(R)$ is the ion potential energy in a screened cluster field. Below, we will consider the following range of distances from the cluster center:

$$\left|U(r_0)\right| \gg \left|U(R)\right| \gg \varepsilon \,. \tag{5.15}$$

Under these conditions, a trapped ion cannot go to infinity and is captured in a finite orbit. If the process of resonant charge exchange proceeds at a distance R from the cluster center and the energy of an incident atom is ε, the probability of transition to a finite orbit for an initially free ion, $P_{tr}(R, \varepsilon)$, and the probability of transition to a finite orbit for an initially bound ion, $p_{tr}(R, \varepsilon)$, are equal to

$$P_{tr}(R, \varepsilon) = p_{tr}(R, \varepsilon) = \int_0^{\cos\theta_0} \mathrm{d}\cos\theta = \cos\theta_0 = \sqrt{1 - \frac{r_0 R_0}{R^2}}, \quad R \geqslant \sqrt{r_0 R_0} \,, \tag{5.16}$$

in accordance with parameters of the process displayed in Fig. 6. Taking into account that a trapped ion can leave the interaction region at the boundary of the cluster field and

become free, we use the following simple model for ion capture:

$$P_{\rm tr}(R,\varepsilon)=\sqrt{1-\frac{r_0R_0}{R^2}}\left(1-\frac{R}{l}\right),\quad l>\sqrt{r_0R_0}\,. \tag{5.17}$$

Let us find the relation between the number densities of free ions ($N_{\rm i}$) and trapped ions ($N_{\rm tr}$) on the basis of the balance equation

$$N_{\rm a}\sigma_{\rm res}N_{\rm i}P_{\rm tr}v_{\rm i}=N_{\rm a}\sigma_{\rm res}N_{\rm tr}v_{\rm tr}(1-p_{\rm tr})\,. \tag{5.18}$$

Here, $v_{\rm i}$ is the relative velocity of a free ion and atom which partake in the resonant charge exchange process, $v_{\rm tr}$ is the same quantity for a bound ion, $P_{\rm tr}$ is the probability of resonant charge exchange for a free ion at the beginning, and $p_{\rm tr}$ is the same quantity for a bound ion. For a distance R from the cluster, where $|U(R)|\gg\varepsilon$, the ion velocity at this distance R from the cluster is $v_{\rm i}=\sqrt{2|U(R)|/m_{\rm i}}$. The kinetic energy of a bound ion in the cluster Coulomb field, according to the virial theorem [128], is equal to $|U(R)|/2$ on average, so that the average velocity of the bound ion is $v_{\rm tr}=\sqrt{|U(R)|/m_{\rm i}}$, and $v_{\rm i}/v_{\rm tr}=\sqrt{2}$. Considering that $P_{\rm tr}=p_{\rm tr}$, from the balance equation (5.18) we obtain the following relation between the number densities of trapped and free ions:

$$N_{\rm tr}(R)=N_{\rm i}(R)\,\frac{R^2\sqrt{2}}{r_0R_0}\sqrt{1-\frac{r_0R_0}{R^2}}\left(1+\sqrt{1-\frac{r_0R_0}{R^2}}\right)\times\left(1-\frac{R}{l}\right),\quad l\gg R\geqslant\sqrt{R_0r_0}\,, \tag{5.19}$$

and the last factor takes into account that trapped ions exist only in the region of action of the cluster field: $R<l$. As is seen, at low number densities of electrons and ions in an ionized gas, the screening of the cluster field is created by trapped ions, whereas at high plasma densities this is due to free ions.

In determining the screening parameters for the cluster charge, we will use a simple algorithm, so that free ions dominate in the field formation in the first version, while the self-consistent field of a charged cluster and surrounding ionized gas is created by trapped ions in the second version. It turns out that the screening parameters are close for these two versions at such plasma densities that the contributions to the cluster field screening from free and trapped ions have the same order of magnitude. Below, we will demonstrate the practicality of this algorithm.

If free ions dominate in the cluster field screening, the simplified potential of the self-consistent cluster field is as follows:

$$U(R)=\frac{z(R)\,e^2}{R}\,,$$

and the number densities of free and trapped ions in the region of cluster field action, in accordance with formulas (5.5), (5.6), and (5.19), are

$$\begin{aligned}N_{\rm i}(R)&=N_0\sqrt{1+\frac{4R_0}{\pi R}\left[1-\left(\frac{R}{l}\right)^{5/2}\right]^2}\,,\\ N_{\rm tr}(R)&=N_{\rm i}(R)\,\frac{2R^2\sqrt{2}}{r_0R_0}\,\Phi(R)\left(1-\frac{R}{l}\right),\\ \Phi(R)&=\frac{1}{2}\sqrt{1-\frac{r_0R_0}{R^2}}\left(1+\sqrt{1-\frac{r_0R_0}{R^2}}\right).\end{aligned} \tag{5.20}$$

In the other limiting case, when trapped ions dominate in the cluster field screening, as we did earlier, we solve the equation for a current charge inside a sphere with radius R, which has the form

$$\frac{{\rm d}z}{{\rm d}R}=-4\pi R^2\,N_{\rm i}(R)\,,$$

with the boundary condition $z(r_0)=|Z|$, but as the number density of ions $N_{\rm i}(R)$ we use the number density of trapped ions. Solving this equation yields

$$z=|Z|\left[1-\left(\frac{R}{l}\right)^{9/2}\right]^2,\quad l=1.05\left(\frac{|Z|\,r_0\sqrt{R_0}}{N_0\Phi(9l/11)}\right)^{2/9}. \tag{5.21}$$

From this it follows that the number densities of free and trapped ions for the second version of screening of the cluster field are given by

$$\begin{aligned}N_{\rm i}(R)&=N_0\sqrt{1+\frac{4R_0}{\pi R}\left[1-\left(\frac{R}{l}\right)^{9/2}\right]^2},\\ N_{\rm tr}(R)&=N_{\rm i}(R)\,\frac{2R^2\sqrt{2}}{r_0R_0}\,\Phi(R)\left(1-\frac{R}{l}\right).\end{aligned} \tag{5.22}$$

The above expressions for the number densities of free and trapped ions allow us to find the parameters of the cluster field screening for the two versions under consideration. Let us define the screening charge due to free ($Q_{\rm i}$) and trapped ($Q_{\rm tr}$) ions according to the formulas

$$Q_{\rm i}=\int_{r_0}^{l}4\pi N_{\rm i}(R)\,R^2\,{\rm d}R\,,\quad Q_{\rm tr}=\int_{\sqrt{r_0R_0}}^{l}4\pi N_{\rm i}(R)\,R^2\,{\rm d}R\,, \tag{5.23}$$

and according to the definition of the radius l of cluster field action we have

$$Q=Q_{\rm i}+Q_{\rm tr}=|Z| \tag{5.24}$$

as the equation for a radius of cluster field action l. Let us define simultaneously the part of the screening charge ξ that is created by trapped ions as

$$\xi=\frac{Q_{\rm tr}}{Q_{\rm i}+Q_{\rm tr}}\,. \tag{5.25}$$

Figure 7 gives the dependence of the part of the screening charge ξ due to trapped ions on the reduced plasma density in accordance with formula (5.25). The number density of ions in the cluster field is defined by formulas (5.20) and (5.22) for these two versions. As is seen, both versions give close results. In particular, the contribution of trapped ions to screening of the cluster field for the example of the argon plasma with the parameters $T_{\rm e}=1$ eV, $T_{\rm i}=400$ K equals $\xi=0.53$ and $\xi=0.50$ at the reduced plasma density $N_0r_0^2=100$ cm^{-1}, if we use formulas (5.20) and (5.22), respectively, for the number densities of ions for the first and second versions.

Figure 8 displays the dependence of the reduced radius of action of the cluster field in an ionized gas on the reduced plasma density according to formula (5.24), in compliance with the two versions under consideration, where the number density of ions is defined by formulas (5.22) and (5.23). On the basis of formulas (5.6) and (5.21), the radii of action of the cluster field $l_{\rm free}$, if free ions dominate in the cluster field

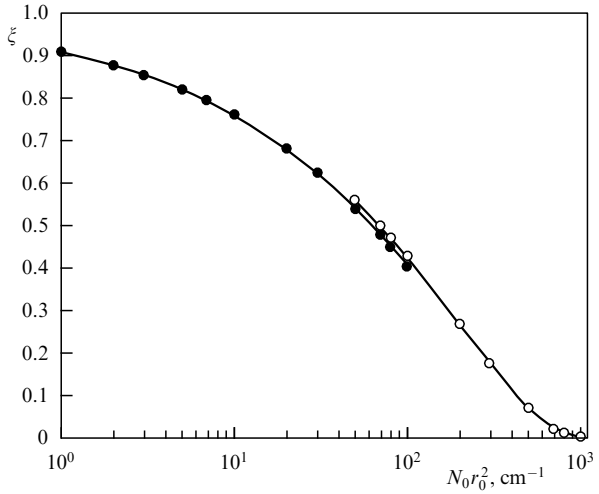

Figure 7. Contribution of trapped ions to charge screening for a cluster located in ionized argon as a function of the reduced number density of electrons and ions, in accordance with formula (5.25) and at the plasma parameters $T_e = 1$ eV, $T_i = 400$ K. White circles relate to the case where free ions dominate in the screening of the cluster charge, and dark circles correspond to the opposite case, when trapped ions dominate in the charge screening.

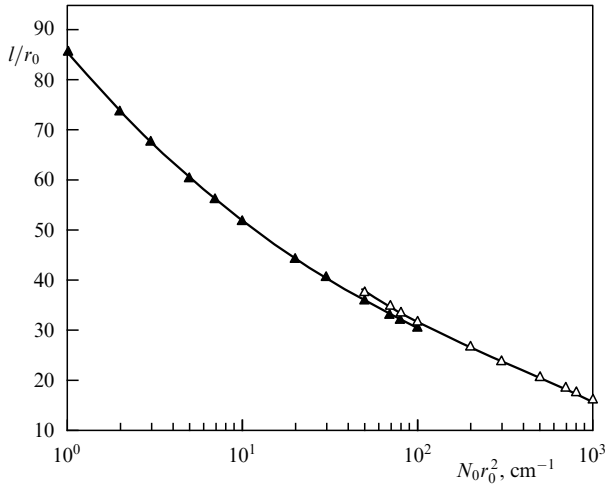

Figure 8. The reduced radius of action of a charged cluster field in an ionized gas in accordance with formula (5.24) as a function of the reduced number density of an argon plasma with parameters $T_e = 1$ eV, $T_i = 400$ *K*. White circles correspond to the version where free ions dominate in the cluster charge screening, and their number density near the cluster is given by formulas (5.20), whereas dark circles relate to the opposite version, where trapped ions dominate, so the number density of ions is determined by formulas (5.22).

screening, and l_{trap}, if trapped ions dominate, are given by formulas

$$\frac{l_{free}}{r_0} = \frac{A}{(N_0 r_0^2)^{2/5}}, \quad \frac{l_{trap}}{r_0} = \frac{B}{(N_0 r_0^2)^{2/9}}, \quad A = 0.66\,\frac{(|Z|/r_0)^{2/5}}{(R_0/r_0)^{1/5}},$$

$$B = \frac{1.05}{\Phi}\left(\frac{|Z|}{r_0}\right)^{2/9}\left(\frac{R_0}{r_0}\right)^{1/9}, \qquad (5.26)$$

where the parameters A and B are independent of a cluster radius r_0. The two versions lead to close results. In particular, for the example of an argon plasma with the parameters $T_e = 1$ eV, $T_i = 400$ K at the reduced number density of ions

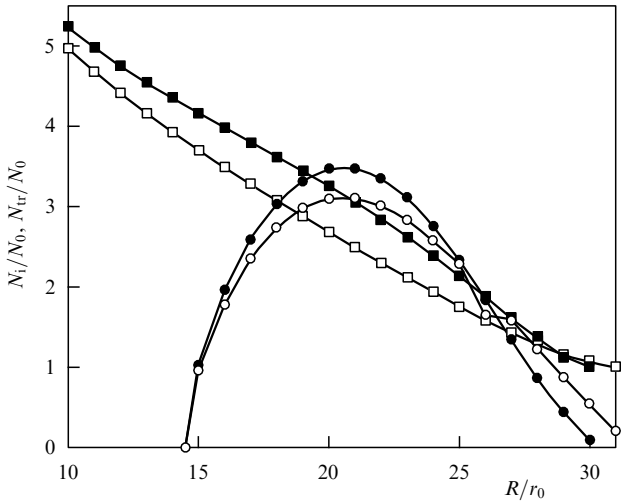

Figure 9. The number density of free ions (squares) and trapped ions (circles) in a self-consistent field of a cluster and surrounding ionized argon with parameters $T_e = 1$ eV, $T_i = 400$ K; the reduced number density of electrons and ions far from the cluster is $N_0 r_0^2 = 100$ cm^{-1}. Dark marks relate to formulas (5.6), and white ones relate to formulas (5.21).

$N_0 r_0^2 = 100$ cm^{-1}, the reduced radius of action of the cluster field, l/r_0, is equal to 28 and 29 for the first and second versions, respectively.

It should be noted that the calculated results depend on the number density N_0 of plasma electrons and ions and the cluster radius r_0 in the form of the combination $N_0 r_0^2$, which was introduced above. The identical contribution of the free and trapped ions to cluster field screening takes place at $N_0 r_0^2 = 100$ cm^{-1}, and the trapped ions disappear at $N_0 r_0^2 \approx 10^3$ cm^{-1} for the example of an argon plasma with the parameters $T_e = 1$ eV, $T_i = 400$ K (see Fig. 7). Figure 9 gives the number densities of free and trapped ions as a function of the reduced distance from the cluster center at the reduced number density $N_0 r_0^2 = 100$ cm^{-1}, whereat the contribution to screening of the cluster charge due to free and trapped ions is comparable.

Thus, for cluster charging in a rarefied ionized gas, the cluster charge is weakly dependent on the screening character, since the flux of ions towards the cluster is generated in a region where the cluster field does not act. Next, because screening of the cluster field proceeds mostly at large distances from the cluster compared with its radius, the cluster potential near it is the Coulomb-like, and the flux of electrons towards the cluster surface is also independent of the screening character. Hence, we obtain a simple equation (5.11) for the cluster charge. But the character of ion screening of the cluster field becomes more complicated because it is determined by both free and trapped ions.

Nevertheless, we have a simple algorithm to solve this problem, since the two versions based on domination of free or trapped ions give close results at values of the parameter $N_0 r_0^2$ where the contributions of free and trapped ions to screening of the cluster field are comparable. This allows us, in particular, to use one of the expressions in formula (5.26) for the radius of action of the cluster field, depending on the basic contribution to screening of the cluster field due to either free or trapped ions. As a result, we have a simple algorithm for determination of the radius of action for the cluster field.

Note that the radius of action of the cluster field in an ionized gas allows us to analyze other aspects of interaction of the charged cluster with a surrounding plasma. For example, an opportunity appears to determine the drag force for an ion in a dusty plasma [101], i.e., the friction force for moving ions. Indeed, a plasma ion is scattered if it penetrates into the region of action of the cluster field, which gives about πl^2 for the diffusion cross section of ion– cluster scattering. The contribution to the friction force of ions in a dusty plasma due to ion scattering on clusters is approximately $N_p \pi l^2 / N_a \sigma^*$, where N_p is the number density of clusters, N_a is the number density of buffer gas atoms, and σ^* is the diffusion cross section of ion–atom scattering.

5.3 Cluster charging in an ionized gas under nonequilibrium conditions

In analyzing the process of cluster charging in a rarefied plasma, we assumed that attachment of electrons and ions to the cluster surface does not contribute to the plasma ionization balance, i.e., there is an intense source of plasma generation and destruction, and the cluster presence in the plasma does not violate the ionization equilibrium. Therefore, we assumed that the number density of electrons and ions at large distances from the cluster compared with a radius of action l of its field tends to the equilibrium value N_0 which is determined by an external source. This condition is more or less fulfilled for a laboratory dusty plasma and is violated for a cosmic plasma. Below, we will analyze some aspects of the plasma interaction with small particles in the limit of a low plasma density.

Based on the above formulas, we will first establish the criterion of a weak screening of the cluster field by ions, where the plasma does not screen the cluster field and it is almost Coulomb-like, i.e., $l = R_0$, and formula (5.19) gives the number density of trapped ions in the form

$$N_{tr}(R) = \frac{4\sqrt{2}}{\sqrt{\pi}} \frac{N_0 R^{3/2}}{r_0 \sqrt{R_0}} \left(1 - \frac{R}{R_0}\right), \quad R_0 \geqslant R \gg \sqrt{R_0 r_0}\,. \tag{5.27}$$

According to formula (5.27), the maximum number density of trapped ions is attained at the distance $R_{max} = 0.6 R_0$ from the cluster, and it is

$$N_{tr}(R) = 0.59 N_0 \frac{R_0}{r_0}\,.$$

As is seen, this value exceeds remarkably the number density N_0 of electrons and ions far from the cluster.

Below, we will establish the criterion of weakness of the cluster charge screening by a surrounding ionized gas. From formula (5.27) it follows that the ion charge Q_{tr} in a sphere of radius R_0 equals

$$Q_{tr}(R_0) = \frac{4\pi\sqrt{2} R_0^4 N_0 e}{r_0} \approx 0.86 \frac{N_0 R_0^4}{r_0}\,.$$

Hence it follows that the criterion of weakness for screening of the cluster charge $Q_{tr} \ll |Z|e$ by a surrounding ionized gas has the form

$$N_0 R_0^3 \ll \frac{T_i r_0}{e^2}\,. \tag{5.28}$$

In particular, for the example of an argon plasma with the parameters $T_e = 1$ eV, $T_i = 400$ K at the cluster radius $r_0 = 1$ μm, we have $R_0 \approx 210$ nm, so that criterion (5.28) gives $N_0 \ll 3 \times 10^5$ cm^{-3}, which testifies to the importance of cluster field screening in a laboratory plasma.

The above consideration is suitable for a nonequilibrium plasma with $T_e \gg T_i$. Indeed, trapped ions are formed in charge transfer collisions in a range of distances from the cluster $\sqrt{r_0 R_0} \leqslant R \leqslant R_0$, and from the lower boundary they are captured on the cluster surface, while they leave the region of action of the cluster field from the upper boundary. The above formulas work better as the difference between the upper and lower boundaries grows. For the equilibrium argon plasma with $T_e = T_i$, the ratio of distances for the boundaries is $\sqrt{R_0/r_0} \approx \sqrt{\ln(m_i/m_e)} \approx 3.3$ in the limit of a low density of surrounding plasma, whereas for the example of argon plasma under consideration, with the parameters $T_e = 1$ eV, $T_i = 400$ K, this ratio builds up to

$$\sqrt{\frac{R_0}{r_0}} = \sqrt{\frac{|Z|e^2}{T_i r_0}} \approx \sqrt{\frac{T_e}{T_i} \ln\left(\frac{m_i}{m_e}\right)} = 18$$

in the limit of a low plasma density.

The above results describe correctly a region of distances from the cluster which are not close to the boundary of action of the self-consistent field of a cluster and ionized gas. In this region in space, the screening of this field is determined by both free and trapped ions. Near the boundary of action of the self-consistent field, where $|U(R)| \sim T_e$, electrons also make a contribution to the cluster field screening. Since the ionization and recombination processes do not contribute to the ionization balance in this region, the screening of the cluster field has the Debye character.

According to the results of Section 5.2, the more rarefied the buffer gas, the larger the charge of a microparticle at a given its size, and the larger the contribution made by trapped ions to the ionic coat that screens the cluster charge. Such conditions are fulfilled in an astrophysical plasma with dust particles, in particular, in the dusty plasma of the Solar system [96, 101, 129], which will be analyzed briefly below. The basis of this plasma is the solar wind [130–132] — the plasma flux consisting of electrons and protons from the solar corona into a surrounding space. Interaction of the solar wind with a dust of comet tails or with a dust from Saturn, Jupiter, or Uranus leads to the formation of a specific dusty plasma, and its interaction with magnetic fields of planets creates specific structures of a dusty plasma, such as the rings of Saturn, Jupiter, and Uranus. The number density of electrons and protons at Earth's level in the solar wind is approximately 7 cm^{-3}, the electron temperature is about 2×10^5 K, the proton temperature reaches 5×10^4 K, and the rate of the plasma flow is 4×10^7 cm s^{-1}.

In particular, the E- and F-rings of Saturn contain ice particles from 0.5 up to 10 μm in size [133, 134], and a typical number density of ice particles is 30 cm^{-3} [133]. The sources of dust particles are the satellites Enceladus for the E-ring [135–137] and Prometheus and Pandora for the F-ring [138]. Simultaneous measurements within the framework of the Cassini project give the above values for parameters of dust particles [139, 140] and plasma parameters [141, 142] for the E-ring. Note that in the above consideration we assumed that far from each particle the number density of electrons and ions is determined by external conditions, and the presence of particles does not influence them. This does not hold true for the astrophysical dusty plasma of the Solar system, where the plasma number density in a region between particles does not

correspond to the plasma density in the solar wind, and for Saturn's E-ring it is $N_0 = 30-100$ cm^{-3}, which exceeds the plasma density of the solar wind on the surface of Saturn. Next, the electron temperature ranges over 10–100 eV [143], with the basic kinds of ions being OH^+ and H_2O^+ at a temperature of 10^3 K.

Let us apply the above results to the dusty plasma of Saturn's E-ring. Taking the parameters of this plasma as $r_0 = 1$ μm, $T_e = 30$ eV, and $T_i = 10^3$ K, on the basis of formula (5.11) we obtain the equilibrium particle charge $|Z| = 2 \times 10^5$, and formula (5.12) gives $R_0 \approx 0.3$ cm. This value is comparable to the distance between nearest neighbors, since the number density of particles is $N_p = 30$ cm^{-3} [133]. This value is also comparable to an ionic coat radius l of a surrounding plasma, because $l \sim R_0$. However, the above cluster charge contradicts observed data. Indeed, the number density of trapped ions is $N_i \sim 10^6$ cm^{-3} at a given number density of particles and the equilibrium particle charge, which is higher than the observable value of $N_0 \approx 10^2$ cm^{-3}. Nevertheless, the latter significantly exceeds the plasma number density in the solar wind, ~ 0.1 cm^{-3}, but the flux of the solar wind plasma cannot provide an equilibrium with the dusty plasma, so that the dusty plasma density is much lower than that under equilibrium conditions. Indeed, if we employ the observable parameters of Saturn'a rings, we obtain the corresponding dusty plasma consisting of negatively charged particles, trapped positive ions, and a solar wind flow that has not completely stopped. Then, the average particle charge is $Z = -3$, and the field size for an individual particle is comparable with its size and is remarkably less than the average distance between nearest particles.

One can consider this problem from another standpoint, so that a dusty plasma is formed as a result of mixing of the solar wind with dust, and the number density of electrons and ions in this plasma is much higher than that in its source, the solar wind. This results from the capture of ions by charged dust particles in finite orbits, which stops the plasma flow, increasing in this manner the number density of charged particles. The same proceeds in a comet plasma [145, 146], where the dusty plasma originates in the comet tail as a result of interaction of the solar wind and a comet dust (see Fig. 10 [144]), and the magnetic field is an important element of this interaction [147]. The plasma density for a comet tail ranges over 10^3-10^4 cm^{-3} [148, 149], if the comet is located at the Earth level, and this remarkably exceeds the plasma density of the solar wind, and the electron temperature of the comet tail $T_e \sim 10^4$ K [149–151] corresponds to the electron temperature in the solar wind. A heightened density of the comet plasma follows from the capture of ions by charged dust particles and the long lifetime of trapped ions.

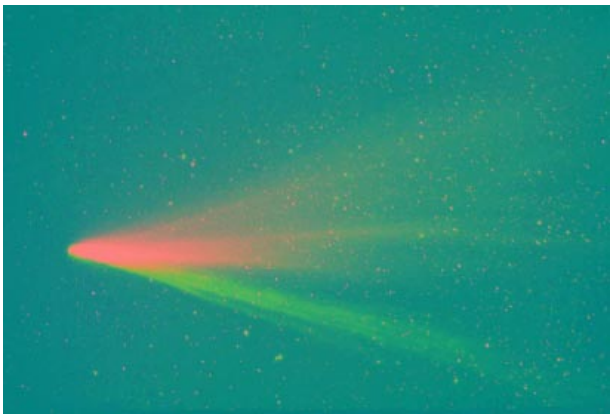

Figure 10. The comet tail consisting of ions and dust particles is separated from the comet nucleus in the direction from the Sun as a result of interaction with a solar wind and magnetic field, so this interaction provides binding of comet nucleus and tail in the course of comet evolution [144].

Thus, the peculiarity in the behavior of a charged dust particle in an astrophysical plasma is concerned with the low density of a surrounding gas, which might lead to the large size of the ionic coat consisting of trapped ions around each particle. But due to a low flux of electrons and ions in the solar wind, this plasma is far from saturation, and the particle charge is lower than the equilibrium charge of dust particles in this plasma.

5.4 Diffusion regime for charging clusters and small particles in an ionized gas

Let us consider attachment of electrons and ions to a cluster in a dense buffer gas if the criterion

$$r_0 \gg \lambda \tag{5.29}$$

holds true, and the attachment rate is restricted by processes of motion of electrons and ions in a space. The cluster charging in an ionized buffer gas results from electron and ion diffusion and drift in the charged cluster field, and the number $J_+(R)$ of ions which intersect the sphere of radius R per unit time is given by

$$J_+ = 4\pi R^2 \left(- D_+ \frac{dN_+}{dR} + K_+ E N_+ \right). \tag{5.30}$$

Here, $N_+(R)$ is the number density of ions, and D_+, K_+ are the respective diffusion coefficient and the mobility of ions in the self-consistent cluster field of strength $E(R)$. Below, we will consider cluster charging in a dense buffer gas within the framework of the Fuks theory [152] based on the assumption of a relatively weak electric field induced near the cluster due to an ionized gas, which corresponds to the criterion

$$r_D \gg r_0 . \tag{5.31}$$

Here, r_D is the Debye–Hückel radius for an ionized gas [102]. Assuming the cluster charge to be negative and equal to $-|Z|e$, we obtain $E(R) = Ze/R^2$ for the electric field strength of the cluster. The absence of ionization and recombination processes near the cluster is an important element of the Fuks theory. One can then consider relation (5.30) as the equation for the number density of ions near the cluster, because the ion current $J_+(R)$ is independent of a radius of a sphere intersected. Connecting the diffusion coefficient D_+ of ions in a buffer gas and their mobility K_+ in a weak electric field by the Einstein relation [81, 82] in accordance with formula (3.15), we have

$$K_+ = \frac{eD_+}{T} ,$$

where T is the gas temperature, and equation (5.30) takes on the form

$$J_+ = -4\pi R^2 D_+ e \left(\frac{dN_+}{dR} - \frac{Ze^2 N_+}{TR^2} \right).$$

Solving this equation with the boundary condition $N_+(r_0) = 0$, we obtain for the number density of ions:

$$N_+(R) = \frac{J_+}{4\pi D_+}\int_{r_0}^{R}\frac{\mathrm{d}R'}{(R')^2}\exp\left(\frac{Ze^2}{TR'}-\frac{Ze^2}{TR}\right) = \frac{J_+T}{4\pi D_+Ze^2}\left[\exp\left(\frac{Ze^2}{Tr_0}-\frac{Ze^2}{TR}\right)-1\right].$$

Using the boundary condition $N_+(\infty) = N_0$ far from the cluster, we obtain the Fuks formula [152] for the rate of ion attachment to the cluster surface:

$$J_+ = \frac{4\pi D_+ N_0 Ze^2}{T\{\exp[Ze^2/(Tr_0)]-1\}}. \tag{5.32}$$

In the limit of a neutral cluster, $Z \to 0$, the Fuks formula (5.32) is transformed into the Smoluchowski formula (2.8) [74] for the attachment rate J_0 of ions or atoms to a neutral cluster of a radius r_0:

$$J_0 = 4\pi D_+ N_0 r_0. \tag{5.33}$$

The Fuks formula (5.32) may also be used for electrons by replacing $Z \to -Z$. In the limiting case, when the cluster charge and those of attaching ions or electrons have the opposite sign and $Ze^2/(r_0T) \gg 1$, the Fuks formula is transformed into the Langevin formula [153]:

$$J_- = \frac{4\pi Ze^2 N_0 D_-}{T} = 4\pi Ze K_- N_0, \tag{5.34}$$

where the cluster charge is assumed positive, and an electron or negative ion attaches to it. Equalizing the attachment rates of electrons and ions to a cluster, we find the cluster charge

$$Z = \frac{r_0 T}{e^2}\ln\frac{K_+}{K_-}. \tag{5.35}$$

Since the mobility of electrons is higher than that for ions, the cluster is negatively charged.

The above expressions for identical temperatures of electrons and ions may be generalized for different electron (T_e) and ion (T_i) temperatures, and the formula for the cluster charge takes then the form [31, 58]

$$Z = \frac{r_0 T_\mathrm{e}}{e^2}\ln\frac{K_+(T_\mathrm{i})}{K_-(T_\mathrm{e})}. \tag{5.36}$$

In the case where the electron distribution function differs from the Maxwell one, it is necessary to use in this formula the quantity $T_\mathrm{e} = eD_-/K_-$ as the electron temperature [31, 58]. We use here the proportionality of the electron drift velocity to the electric field strength, which holds true at not high electric field strengths. Note also that formula (5.35) is valid at large values of the cluster charge because the assumption is used implicitly that attachment of an electron or ion to a cluster, which corresponds to a change in the cluster charge by unity, weakly influences the interaction of the charged cluster with a surrounding plasma.

In order to ascertain the character of screening of the cluster field by plasma electrons and ions, we introduce the reduced potential energy for an electron. Assuming a negative cluster charge Z and an identical temperature of electrons and ions, we have for the reduced potential energy at the cluster surface: $\xi(r_0) = \xi_0 = \ln(K_-/K_+)$. It should be noted that the Fuks formula (5.32) relates to the positive cluster charge, while for an ionized gas consisting of electrons and ions it is negative, i.e., $\xi = |Z|e^2/(RT)$, where R is a distance from the cluster, so that $\xi_0 \geqslant \xi \geqslant 0$. Taking this into account in the above formulas, we obtain the number densities of ions and electrons:

$$N_\mathrm{i}(R) = N_0\left[\frac{\exp(\xi_0)-\exp(\xi)}{\exp(\xi_0)-1}\right], \qquad N_\mathrm{e}(R) = N_0\left[\frac{\exp(\xi_0-\xi)-1}{\exp(\xi_0)-1}\right], \tag{5.37}$$

and the reduced difference in the number densities of ions and electrons is expressed as

$$n(\xi) \equiv \frac{N_\mathrm{i}(R)-N_\mathrm{e}(R)}{N_0} = \frac{[1-\exp(\xi-\xi_0)][1-\exp(-\xi)]}{1-\exp(-\xi_0)}. \tag{5.38}$$

Figure 11 displays the function $n(\xi)$ that is symmetric with respect to transformation $\xi \to \xi_0 - \xi$, and has the maximum at $\xi = \xi_0/2$:

$$n_\mathrm{max} = \frac{1-\exp(-\xi_0/2)}{1+\exp(-\xi_0/2)}. \tag{5.39}$$

As is seen, $n(\xi) \leqslant 1$, and at low ξ we have $n(\xi) = \xi$.

The above expressions are valid in a distance range where screening of the cluster charge by a surrounding ionized gas is weak, so the Coulomb field of the cluster field acts at these distances. This is valid under the condition

$$r_0 \ll r_\mathrm{D}, \quad r_\mathrm{D} = \sqrt{\frac{T}{4\pi Z N_0 e^2}}, \tag{5.40}$$

where the Debye–Hückel radius r_D relates to identical temperatures T of electrons and ions. In particular, the electron and ion number densities $N_\mathrm{i} = 10^{10}$ cm^{-3}, and the temperature $T = 400$ K corresponds to the Debye–Hückel

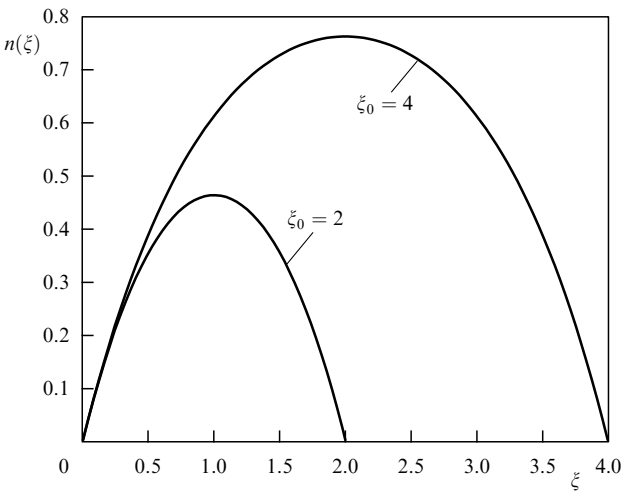

Figure 11. Reduced difference in the number densities of ions and electrons as a function of the reduced potential of the self-consistent field of the charged cluster and surrounding ionized gas.

radius $r_D = 10$ μm, and from this it follows that the conditions of validity of the Fuks concept may both be fulfilled and violated for real cluster sizes and parameters of an ionized gas. If criterion (5.40) ($r_0 \ll r_D$) holds true, the potential of the charged cluster at large distances behaves as

$$\varphi(R) = \frac{Ze}{R} \exp\left(-\frac{R}{r_D}\right), \tag{5.41}$$

which means that screening the cluster charge by electrons and ions of an ionized gas is inessential near the cluster. At high number densities of electrons and ions, this condition is violated, which requires the generalization of the Fuks theory to a high plasma number density. Recently, this effort has been made repeatedly in the study of dusty plasmas (for example, see papers [154–158]), but additional assumptions in these cases prevent the results from applying to real systems.

6. Character of cluster growth in a buffer gas

6.1 Conversion of atomic vapor into a gas of clusters in a buffer gas

Figure 12 represents schematically the basic mechanisms of cluster growth in a buffer gas. Starting from the 19th century, these processes have been studied for other systems and media, which explains the terms used in describing these processes. Below, we will be guided by a system consisting of a buffer gas and metal vapor that is partially or fully converted into metal clusters. For simplicity, clusters are assumed to be liquid and consisting of a large number of atoms, so that each cluster is a spherical liquid drop cut out of a bulk liquid (see Section 2). The number densities of atoms in the cluster and bulk liquid are identical.

The first mechanism of cluster growth in Fig. 12 corresponds to the partial or complete conversion of an atomic vapor into a gas of clusters. Then formation of nuclei of condensation is the first stage of this process, and the subsequent cluster growth results from attachment of free atoms to them, as was considered in Section 4.1. Then, realization of the kinetic or diffusion regime of cluster growth is determined by the concentration of metal atoms in a buffer gas in accordance with criterion (4.6) or with the opposite criterion.

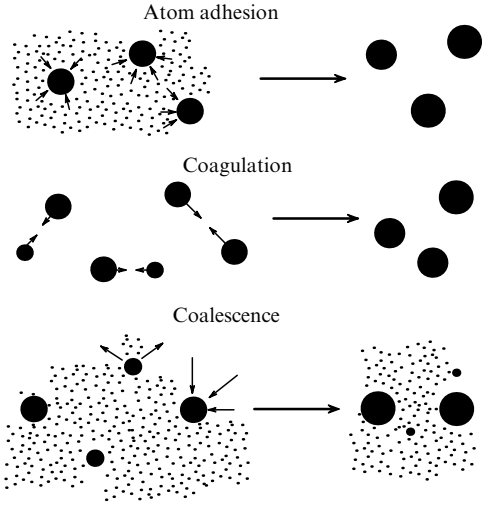

Figure 12. The mechanisms of nucleation and growth of clusters.

Growth of metal clusters under given conditions starts from the formation of condensation nuclei and depends on the character of this process. Below, we will consider the growth of metal clusters if at the beginning the metal is found in the state of an atomic vapor. Then, the processes of formation and growth of clusters proceed according to the scheme [159, 160]

$$A + 2M \to A + M_2\,, \quad M_n + M \to M_{n+1}\,, \tag{6.1}$$

where A is a buffer gas atom, and M is a metal atom.

Let us consider the kinetic regime of cluster growth. The growth of an individual cluster as a result of the attachment of metal atoms to it was analyzed in Section 4.1, and for the determination of the size distribution function of clusters, the character of formation of condensation nuclei, i.e., the first process in scheme (6.1), must be taken into account. It is of importance that the formation process of condensation nuclei, i.e., the first process in chemical formulas (6.1), results from three-body collisions of metal atoms with buffer gas atoms and, hence, this process is slow compared to subsequent cluster growth processes. As a result, small clusters are practically absent in the size distribution function of clusters. This position is governed by the parameter

$$G = \frac{k_0}{KN_a} \gg 1\,, \tag{6.2}$$

where k_0 is the reduced rate constant of atom–cluster collision, given by formula (2.5), K is the rate constant of the three-body process, the first process in scheme (6.1), and N_a is the number density of buffer gas atoms. Since a typical value of the reduced rate constant of atom–cluster collision is $k_0 \sim 10^{-9}$ cm^3 s^{-1}, and the rate constant of the three-body process lies in the range of $K \sim 10^{-33} - 10^{-32}$ cm^6 s^{-1}, parameter (6.2) is large enough, $G \sim 10^3$, even at atmospheric pressure. This means that the process of formation of new condensation centers is relatively weak, and large clusters are formed even at the beginning. Under such conditions, the parameters of complete transformation of an atomic metal vapor into a gas of metal clusters are as follows [31, 58, 161]:

$$\overline{n} = 1.2G^{3/4}\,, \quad \tau_{cl} = \frac{3.2G^{1/4}}{N_m k_0}\,. \tag{6.3}$$

Here, $\overline{n}$ is the average number of cluster atoms after complete conversion of atomic vapor into a gas of clusters in a buffer gas, and τ_{cl} is the time of this conversion.

The kinetic regime of conversion of an atomic metal vapor into a gas of clusters in a buffer gas requires the validity of the criterion opposite to criterion (4.6), which has the form

$$N_m \lambda^3 \gg 1\,. \tag{6.4}$$

Criterion (6.4) relates to a high concentration $c_m = N_m/N_a$ of metal atoms in a buffer gas, where N_m is the number density of metal atoms, N_a is the number density of buffer gas atoms, and the criterion of the kinetic regime of cluster growth has the form

$$c_m \gg N_a^2 \sigma_g^3\,, \tag{6.5}$$

where σ_g is the gas-kinetic cross section for collision of a metal atom and a buffer gas atom.

Let us consider the diffusion regime of cluster growth from an atomic vapor that corresponds to a low concentra-

tion of metal atoms in accordance with criterion (4.6). Then, according to the Smoluchowski formula (2.8), the variation of the average number of cluster atoms $\overline{n}$ is described by the equation

$$\frac{\mathrm{d}\overline{n}}{\mathrm{d}t} = k_\mathrm{m} N_\mathrm{m} \overline{n}^{1/3}\,, \quad k_\mathrm{m} = 4\pi D_\mathrm{m} r_\mathrm{W}\,. \tag{6.6}$$

One can see an analogy with the kinetic regime of cluster growth, but another dependence is observed for the growth rate on the number of cluster atoms; the quantity k_m is now an analog of the reduced rate constant of atom–cluster collisions. Therefore, we construct, as earlier, the parameter that characterizes a large rate of cluster growth in pair atom–cluster collisions, compared with the rate of formation of new condensation nuclei. This parameter is given by

$$g = \frac{k_\mathrm{m}}{K N_\mathrm{a}} \gg 1\,, \tag{6.7}$$

and $g \gg 1$ under the considered conditions.

For determining the rate constant of cluster growth, equation (6.6) is supplemented with the balance equations for the number density N_m of metal atoms and the number density N_cl of clusters, so that the bound atom number density in clusters is $N_\mathrm{b} = N_\mathrm{cl}\overline{n}$. These equations have the form

$$\frac{\mathrm{d}N_\mathrm{m}}{\mathrm{d}t} = -k_\mathrm{m} N_\mathrm{m} N_\mathrm{cl}\, \overline{n}^{1/3}\,, \quad \frac{\mathrm{d}N_\mathrm{cl}}{\mathrm{d}t} = K N_\mathrm{a} N_\mathrm{m}^2\,, \tag{6.8}$$

where K is the rate constant of the first process in scheme (6.1), i.e., the rate constant of three-body formation of condensation nuclei, namely, diatomic metal molecules.

Let us use the simplified solution to the set of equations (6.6), (6.8), assuming the number density N_m of free metal atoms to be constant in the course of cluster growth, and this growth finishes when the number density of bound atoms attains the initial number density of free metal atoms, $N_\mathrm{cl}\overline{n} = N_\mathrm{m}$. This allows us to find the parameters of conversion of a metal vapor into a gas of clusters depending on the parameter g. The average number of cluster atoms $\overline{n}$ at the end of the conversion process and the characteristic time τ_cl of this process are given by

$$\overline{n} \sim g^{3/5}\,, \quad \tau_\mathrm{cl} \sim \frac{g^{2/5}}{k_\mathrm{m} N_\mathrm{m}}\,. \tag{6.9}$$

Note that the parameter g is large when the process of conversion of an atomic metal vapor into a gas of clusters proceeds in a dense buffer gas. In particular, at atmospheric pressure we have $k_\mathrm{m} \sim 10^{-8}$ cm^3 s^{-1}, which gives $g \sim 10^5$, and this value increases with a decrease in the number density N_a of buffer gas atoms as $g \sim N_\mathrm{a}^{-2}$. Thus, the diffusion regime of cluster growth, like the kinetic regime, leads to a large cluster size at the end of the cluster growth process.

6.2 Kinetic regime of cluster coagulation

According to the definition, cluster coagulation is the growth of liquid drops located in a neutral medium (here in a buffer gas) as a result of their joining at the contact. Considering clusters as drops, we have the following scheme of their coagulation:

$$M_{n-m} + M_m \to M_n\,, \tag{6.10}$$

where M is a cluster atom. Atmospheric processes of water condensation and growth of water drops, as well as the processes of mist formation and air pollution, are based on the coagulation process involving liquid particles [21, 162–164]. For definiteness, we will consider below the coagulation process as a result of joining of liquid metal drops located in a buffer gas. In contrast to the above processes of the cluster– buffer gas interaction, the separation of the two regimes of the coagulation process, kinetic and diffusion, takes place here in two ways, relating both to the character of motion of an individual cluster in a buffer gas and to the relative motion of two colliding clusters in a buffer gas.

We first consider the criteria of the kinetic and diffusion regimes of coagulation with respect to approach of two clusters. The diffusion regime of the approach of two clusters requires the fulfillment of the criterion

$$N_\mathrm{cl} \Lambda^3 \ll 1\,, \tag{6.11}$$

where N_cl is the number density of clusters, and Λ is the mean free path of clusters in a buffer gas with respect to a change in their motion directions, and the latter is determined by formula (3.13). The number density of clusters equals $N_\mathrm{cl} = N_\mathrm{b}/\overline{n}$, where N_b is the number density of bound cluster atoms, and $\overline{n}$ is the average number of cluster atoms. Let us single out in criterion (6.11) the dependence on the number density N_a of buffer gas atoms and a typical number n of cluster atoms. We introduce the concentration $c_\mathrm{b} = N_\mathrm{b}/N_\mathrm{a}$ of bound atoms in formula (3.13) for the mean free path Λ of clusters. Criterion (6.11) for the diffusion regime of cluster approaching takes the form

$$N_\mathrm{a} n^{3/4} \gg \left(\frac{c_\mathrm{b}}{\sigma_\mathrm{cl}^3}\right)^{1/2}, \quad \sigma_\mathrm{cl} = \frac{4}{3}\sqrt{\frac{m}{m_\mathrm{a}}}\, r_\mathrm{W}^2\,, \tag{6.12}$$

where m is the mass of a buffer gas atom, m_a is the metal atom mass, and r_W is the Wigner–Seitz radius for this cluster. In particular, in the case of liquid copper clusters located in argon we have $\sigma_\mathrm{cl} = 2.3 \times 10^{-16}$ cm^2, and at the concentration $c_\mathrm{b} = 0.01$ of bound copper atoms in argon criterion (6.12) for the diffusion regime of cluster approach takes the form $N_\mathrm{a} n^{3/4} \gg 3 \times 10^{23}$ cm$^{-3}\sqrt{c_\mathrm{b}}$. According to this estimate, both the kinetic and diffusion regimes of cluster approach are possible in reality. Moreover, as the cluster grows, a transition is possible from the kinetic regime of cluster approach to the diffusion one.

Based on scheme (6.10) of cluster coagulation, one can connect the rate of cluster growth with the rate constant of pair cluster collisions in the form of the Smoluchowski equation [165], independently of the coagulation regime:

$$\frac{\partial f_n}{\partial t} = -f_n \int k(n,m)\, f_m\, \mathrm{d}m + \frac{1}{2}\int k(n-m,m)\, f_{n-m} f_m\, \mathrm{d}m\,. \tag{6.13}$$

Here, $k(n-m,m)$ is the rate constant of process (6.10). The factor $1/2$ accounts for the fact that collisions of clusters consisting of $n-m$ and m atoms are included in this equation twice, and the size distribution function f_n of clusters is normalized by the condition $\int f_n\, \mathrm{d}n = N_\mathrm{cl}$, where N_cl is the number density of clusters.

Introducing the number density $N_\mathrm{b} = \int_0^\infty n f_n\, \mathrm{d}n$ of bound atoms in clusters, one can prove that this quantity does not vary in the course of coagulation. Indeed, multiplying the Smoluchowski equation (6.13) by n and integrating it over

$\mathrm{d}n$, we obtain

$$\frac{\mathrm{d}N_\mathrm{b}}{\mathrm{d}t} = -\int nk(n,m) f_n \,\mathrm{d}n f_m \,\mathrm{d}m + \frac{1}{2}\int nk(n-m,m) f_{n-m} f_m \,\mathrm{d}n \,\mathrm{d}m ,$$

with $n > m$ in the second integral. Replacing $n - m$ by n on the right-hand side of the above equation, we find that the terms on the right-hand side of this equation are cancelled mutually, and the equation takes the form $\mathrm{d}N_\mathrm{b}/\mathrm{d}t = 0$, i.e., within the framework of the Smoluchowski equation the total number density of bound atoms does not vary in the course of cluster coagulation.

For simplicity, we will assume that the rate constant of joining two clusters is independent of cluster sizes, and hence $k(n,m) = k_\mathrm{as}$. Then, the Smoluchowski equation (6.13) takes the form

$$\frac{\partial f_n}{\partial t} = -k_\mathrm{as} f_n \int_0^\infty f_m \,\mathrm{d}m + \frac{1}{2} k_\mathrm{as} \int_0^n f_{n-m} f_m \,\mathrm{d}m .$$

Multiplying this equation by n^2 and integrating with respect to n, we obtain

$$\frac{\mathrm{d}}{\mathrm{d}t}\int_0^\infty n^2 f_n \,\mathrm{d}n = \frac{\mathrm{d}\overline{n}}{\mathrm{d}t} = -k_\mathrm{as}\int_0^\infty n^2 f_n \,\mathrm{d}n \int_0^\infty f_m \,\mathrm{d}m + \frac{1}{2} k_\mathrm{as}\int_0^\infty n^2 \,\mathrm{d}n \int_0^n f_{n-m} f_m \,\mathrm{d}m = \frac{1}{2} k_\mathrm{as} N_\mathrm{b} ,$$

where the average cluster size $\overline{n}$ is defined as

$$\overline{n} = \frac{\int_0^\infty n^2 f_n \,\mathrm{d}n}{\int_0^\infty n f_n \,\mathrm{d}n} ,$$

and the equation for its variation in time has the form

$$\frac{\mathrm{d}\overline{n}}{\mathrm{d}t} = \frac{1}{2} k_\mathrm{as} N_\mathrm{b} . \tag{6.14}$$

The solution of this equation gives the average cluster size

$$\overline{n} = \frac{1}{2} k_\mathrm{as} N_\mathrm{b} t , \tag{6.15}$$

if at the beginning the cluster is relatively small.

Let us determine the size distribution function of clusters under the condition that the rate constant of joining of two clusters in pair collisions is independent of the cluster size. Instead of the size distribution function f_n, it is convenient to use the concentration c_n of clusters of a given size defined as $c_n = f_n/N_\mathrm{b}$, where N_b is the total number density of cluster bound atoms. For the concentration of clusters, we have the normalization condition $\sum n c_n = 1$, and the kinetic equation (6.13) in terms of the cluster concentrations takes the form

$$\frac{\partial c_n}{\partial \tau} = -c_n \int_0^\infty c_m \,\mathrm{d}m + \frac{1}{2}\int_0^n c_{n-m} c_m \,\mathrm{d}m , \tag{6.16}$$

where the reduced time is $\tau = N_\mathrm{b} k_\mathrm{as} t$. This equation has the following solution

$$c_n = \frac{4}{\overline{n}^2} \exp\left(-\frac{2n}{\overline{n}}\right) . \tag{6.17}$$

This expression satisfies the normalization condition $\int_0^\infty n c_n \,\mathrm{d}n = 1$ and formula (6.15) for the average cluster size $\overline{n}$. Indeed, substituting expression (6.17) into the kinetic equation, we obtain formula (6.15) in the form $\overline{n} = \tau$.

The above expressions are valid for both the kinetic and the diffusion regimes of coagulation and are based on the assumption that the rate constant of joining of two clusters in pair collisions is independent of the cluster size. Below, we will use these relations in the analysis of the kinetic regime of coagulation in cluster growth based on formulas (2.6) and (2.7) for the rate constant of cluster association that depends weakly on the cluster size. Substituting expression (2.6) for the rate constant of association of two clusters into equation (6.14), and averaging this rate constant with distribution function (6.17), we obtain the following equation for the rate of variation of the average cluster size due to the coagulation process in the kinetic regime of cluster collision:

$$\frac{\mathrm{d}\overline{n}}{\mathrm{d}t} = k_0 N_\mathrm{b} I \,\overline{n}^{1/6} , \quad I = \frac{1}{2}\int_0^\infty \int_0^\infty (x^{1/3} + y^{1/3})^2 \sqrt{\frac{x+y}{xy}} \times \exp(-2x - 2y)\, x \,\mathrm{d}x y \,\mathrm{d}y = 5.5 . \tag{6.18}$$

This leads to the following expression for variation of the average cluster size in time [166, 167]:

$$\overline{n} = 6.3(N_\mathrm{b} k_0 t)^{1,2} . \tag{6.19}$$

Since $n \gg 1$, this formula holds true under the condition

$$k_0 N_\mathrm{b} t \gg 1 .$$

Returning to the problem of cluster growth in a buffer gas, we will prove that transformation of an atomic metal vapor into a gas of clusters is separated in time from the subsequent process of cluster growth due to coagulation, i.e., a typical time of coagulation in the kinetic regime exceeds significantly a characteristic time of transformation of a metal vapor into clusters. Indeed, considering the transformation of an atomic metal vapor into a gas of metal clusters according to scheme (6.1), we assume that parameter (6.2) is large. When all the metal atoms are converted into clusters, their average size according to formula (6.3) is $\overline{n} \sim G^{3/4}$, and a time of this process is $\tau_\mathrm{at} \sim G^{1/4}/(N_\mathrm{b} k_0)$, where N_b is the number density of bound atoms in clusters. According to formula (6.19), a typical time of an increase in cluster size as a result of coagulation is given by

$$\tau_\mathrm{coag} \sim \frac{\overline{n}^{5/6}}{N_\mathrm{b} k_0} \sim \frac{G^{5/8}}{N_\mathrm{b} k_0} .$$

Taking the average cluster size as obtained after transformation of an atomic metal vapor into a gas of clusters, we obtain the ratio of the time τ_coag of subsequent coagulation to a typical time τ_at for cluster formation from atoms:

$$\frac{\tau_\mathrm{coag}}{\tau_\mathrm{at}} \sim G^{3/8} .$$

Thus, since $G \gg 1$, the processes of transformation of an atomic metal vapor into a gas of clusters and subsequent cluster coagulation are separated in time.

6.3 Diffusion regime of cluster coagulation

The diffusion regime of cluster coagulation with respect to cluster approach is realized under criterion (6.11) and, in contrast to the kinetic regime, has two subregimes. Indeed, the rate constant of joining of two clusters according to

formula (2.9) is expressed through the diffusion coefficient of clusters in a buffer gas, and diffusion of clusters in a buffer gas proceeds either in the kinetic or in the diffusion regime, depending on the cluster size. Thus, the kinetic regime of cluster coagulation with respect to their approach requires a criterion opposite to that in formula (6.12), which has the form

$$N_a n^{3/4} \ll \left(\frac{c_b}{\sigma_{cl}^3}\right)^{1/2}, \quad \sigma_{cl} = \frac{4}{3}\sqrt{\frac{m}{m_a}} r_W^2, \tag{6.20}$$

and the equation (6.14) of cluster growth due to coagulation includes the rate of cluster association according to formula (2.9). We are based on formulas (3.16) for the diffusion coefficient of clusters in a buffer gas in the kinetic and diffusion regimes. Assuming that nearby cluster sizes make the main contribution to the rate of cluster association, we find the respective expressions for the rate constant of association in the kinetic and diffusion regimes of cluster diffusion in a buffer gas:

$$\begin{aligned} k_{as} &= 3\sqrt{\frac{2\pi T}{m}}\,\frac{1}{N_a r_0}, \quad r_0 \ll \lambda, \\ k_{as} &= \frac{8T}{\pi\eta}, \quad r_0 \gg \lambda. \end{aligned} \tag{6.21}$$

For definiteness, let us calculate the parameters of growth of SiO_2 clusters in the region of combustion of SiH_4 and methane CH_4 in atmospheric air using the typical parameters of this process [168]. This process proceeds at atmospheric pressure according to the scheme

$$\begin{aligned} 0.1SiH_4 + 0.9CH_4 + 2O_2 + 8N_2 \\ \rightarrow 0.1SiO_2 + 0.9CO_2 + 2H_2O + 8N_2, \end{aligned} \tag{6.22}$$

and at the temperatures above 2000 K, i.e., above the melting point of SiO_2 [169], growth of the liquid cluster occurs. Under these parameters, the number density of buffer gas molecules is $N_a = 4 \times 10^{18}$ cm^{-3}, and since the Wigner–Seitz radius for SiO_2 is $r_W = 2.2$ Å, and the concentration of SiO_2 molecules under these conditions is $c_b = 0.01$, the criterion for the diffusion regime of cluster coagulation with respect to their approach is $r_0 \gg 1$ nm. Under these conditions, the mean free path of nitrogen molecules, the basic component of air, is $\lambda \sim 1$ μm, and the kinetic regime of cluster diffusion in air is valid if $r_0 \ll 1$ μm.

Solving equation (6.14) for cluster growth with the use of formula (6.21) for the rate constant of cluster association, we obtain the typical number of cluster atoms n over time t for the diffusion regime of cluster approach and the kinetic regime of cluster diffusion in a buffer gas:

$$n = \left(\frac{2v_{ef}\, c_b t}{3}\right)^{3/4}, \quad v_{ef} = \frac{3}{r_W}\sqrt{\frac{2\pi T}{m}}, \quad r_0 \ll \lambda, \tag{6.23}$$

where c_b is the concentration of bound silicon atoms in a buffer gas, v_{ef} is the reduced rate of cluster joining equal to $v_{ef} = 2.6 \times 10^{13}$ s^{-1} under given conditions. Since a typical time of cluster residence in a flame is in the range of 0.01–0.1 s [168], the cluster radius according to formula (6.23) at the end of this process is 45–80 nm. This size corresponds to the kinetic regime of cluster motion in a buffer gas, as was used above.

6.4 Cluster–cluster regime of fractal cluster growth

Coagulation of liquid clusters leads to the transformation of two liquid drops after their contact into one compact drop. If colliding clusters are solid, each of them conserves its form after the contact, but the chemical bond is formed at the contact points. The subsequent growth of such a structure leads to the formation of a fractal aggregate [170]. Under these conditions, the growth of structures corresponds to the cluster–cluster aggregation mechanism [171, 172], where the growth results from the subsequent joining of solid particles into fractal aggregates, and then the joining of small fractal aggregates into larger ones. The fractal aggregate resulting from this process is friable, and its density drops with increasing size. Usually, a fractal aggregate is modelled as consisting of identical solid monomers, and neighboring monomers form chemical bonds at their contact points [173–177]. Fractal properties characterize the correlation in positions of individual solid particles [178, 179] and are described by the fractal dimensionality D, which is the density parameter of such a system. The mass M of particles located in a sphere of radius R with a particle in the center of the sphere is given by

$$M = m_0\left(\frac{R}{a}\right)^D,$$

where m_0 is the mass of an elemental particle, a is its radius, and D is the fractal dimensionality of this aggregate. Note that for a compact aggregate that is fully occupied by particles we have $D = 3$. Since the standard notation for the fractal dimensionality D coincides with the notation of the diffusion coefficient, we will denote below the fractal dimensionality as α. For the number of monomers n constituting the fractal aggregate, the above formula yields

$$n = \left(\frac{R}{a}\right)^\alpha, \tag{6.24}$$

where R is the average radius of the fractal aggregate.

The fractal dimensionality of the aggregate may be determined by modeling a certain process of its growth. We note that, because the fractal aggregate is a random system, fractal aggregates obtained due to the same scenario may have different fractal dimensionalities. Below, we will evaluate the accuracy of determining the fractal dimensionality [175, 180] obtained on the basis of computer simulations [181–186]. In all the simulations, the sticking probability, i.e., the probability of formation of chemical bonds between two contacting small particles, is assumed to be one.

We will give below the results of statistical averaging of fractal dimensionalities based on calculations [181–186]. For the kinetic regime of aggregate growth, i.e., if clusters being joined move along straightforward trajectories, the average of the fractal dimensionality is $\alpha = 1.93 \pm 0.06$, and in the diffusion regime of aggregate growth, i.e., for Brownian motion of clusters in a buffer gas in the course of their joining, the fractal dimensionality equals $\alpha = 1.77 \pm 0.03$. This is in accordance with the fractal dimensionality $\alpha = 1.77 \pm 0.10$ of gold fractal aggregates that are formed in a solution and then placed on a lattice for analysis, as illustrated in Fig. 13.

We now analyze the growth of fractal aggregates in the kinetic regime. The growth rate of fractal aggregates is given by formula (6.18), and we assume the rate constant of cluster association to be independent of their sizes. Formula (6.18)

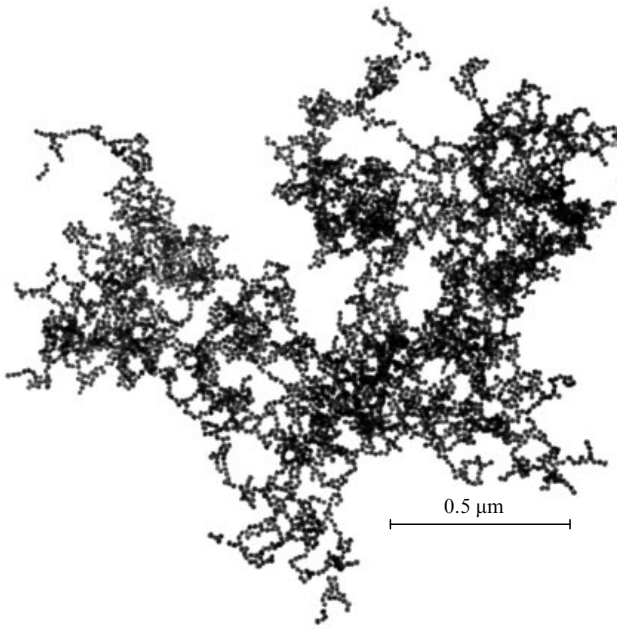

Figure 13. Fractal aggregate.

then takes the form

$$\frac{\mathrm{d}\overline{n}}{\mathrm{d}t} = 5.5k_0 N_\mathrm{b}\,\overline{n}^{\,1/6}\,, \quad k_0 = \sqrt{\frac{8T\pi}{m_\mathrm{p}}}\,r_\mathrm{p}^2\,, \tag{6.25}$$

where m_p is the mass of an elemental particle in the fractal aggregate, and r_p is its radius.

We analyze the character of growth of fractal aggregates under the assumption that the first stage, with chemical processes and nucleation of atomic particles, proceeds rather fast, and liquid particles result from this stage. When the forming particles move outside a hot region (or the melting point of particles increases with increasing size), the particles become solid and subsequently form fractal aggregates. Next, in the course of collisions between fractal aggregates, their size increases, and this process proceeds until fractal aggregates remain in a given region. In the analysis of growth of fractal aggregates, we will take into account that this stage of particle growth proceeds slowly compared to the first stage leading to the formation of solid particles as the basis of the fractal aggregates.

We use the Smoluchowski formula (2.8) for the balance of the number n of monomers which constitute the fractal aggregate, and formula (2.9) gives for the rate constant of association of two fractal aggregates:

$$k_\mathrm{ag} = 4\pi(D_1 + D_2)(R_1 + R_2)\,, \tag{6.26}$$

where D_1, D_2 are the diffusion coefficients of joining fractal aggregates in a buffer gas, and R_1, R_2 are their radii. The balance equation then assumes the form

$$\frac{\mathrm{d}n}{\mathrm{d}t} = k_\mathrm{ag} N_\mathrm{ag}\,, \tag{6.27}$$

where the rate constant k_ag of association of two aggregates is given by formula (6.26), and N_ag is the current number density of fractal aggregates.

Kinetics of the growth of fractal structures for the cluster–cluster character of particle joining [187] is similar to the coagulation growth of liquid clusters, but the number of particles-monomers in the fractal aggregate is now given by formula (6.24) instead of formula (2.1) for liquid particles. Using this analogy, we are dealing with an averaged fractal aggregate that is modelled by a spherical particle. In addition, we assume that the interaction of a fractal aggregate with a buffer gas proceeds on the aggregate surface, as is the case with clusters, and the hydrodynamic radius of the fractal aggregate coincides with its geometric radius. One more peculiarity is that the growth of fractal aggregates due to their porous structure proceeds faster than in the case of compact clusters. Moreover, because the density of fractal aggregates drops as they grow, an aerogel may form at a certain stage of the growth process, which is a structure consisting of particles-monomers and occupying all the space.

For a demonstration of this regime of cluster growth, we return to the above example of the formation of silicon dioxide in a flame (see Section 6.3). Under the above-indicated parameters of combustion of CH_4 and SiH_4 in air at atmospheric pressure, the combustion products go to the chamber, where this mixture is cooled to room temperature. Next, fractal aggregates are formed as a result of the joining of solid particles, and the dynamics of aggregate growth is the same as in the case of compact clusters. We assume, in accordance with the above estimation, that solid clusters (monomers of silicon dioxide) are formed at the first stage with a typical radius $a = 40$ nm and a particle mass $m_0 = 6 \times 10^{-16}$ g, which corresponds to the monomer number density $N_\mathrm{b} = 4.5 \times 10^{10}$ cm^{-3} at the concentration $c_\mathrm{b} = 0.01$ of bound silicon atoms. Being guided by the diffusion regime of motion of fractal aggregates in atmospheric air, we obtain according to formula (6.21) the rate constant of fractal association, $k_\mathrm{as} = 8T/(\pi\eta) = 6 \times 10^{-10}$ cm^3 s^{-1}, which allows us to analyze the character of growth of fractal aggregates on the basis of formula (6.27).

It should be noted that the formation of fractal aggregates is a nonequilibrium process, with the formation of monomers at the first stage, and these monomers subsequently constitute fractal aggregates. In the above example, the first stage proceeds in the region of methane combustion, and a high temperature in this region leads to the fast chemical process. Monomers formed in the hot region subsequently join into fractal aggregates, and a typical time at this stage is several orders of magnitude more than a typical time of monomer formation. Another example of the formation of fractal aggregates in a gas is connected with the first stage proceeding in a plasma torch [188, 189] that results from irradiation of a metal surface by a power pulse laser beam. In this case, due to a small size of a hot region, a time of formation of monomers decreases and a typical monomer size is less than that in a previous case and equals about 10 nm. Therefore, various methods are possible for formation of fractal aggregates in a gas, whose basis are various methods of generation of cluster-monomers [13].

Since the number density of monomers drops in the course of growth of fractal aggregates, the joining of monomers may ultimately lead to formation of an aerogel that occupies all the space. In the case of formation of an aerogel of silicon dioxide, the correlation radius R_c [190–192] (that is, the radius of fractal aggregates when they touch each other and form a continuous structure — aerogel) is equal to 0.4 mm. A typical time of formation of this aerogel, where the density of silicon dioxide is $\rho = 3 \times 10^{-5}$ g cm^{-3}, is approximately 10 days. But, if aerogel growth proceeds in an external electric field, the growth process accelerates and leads to formation of

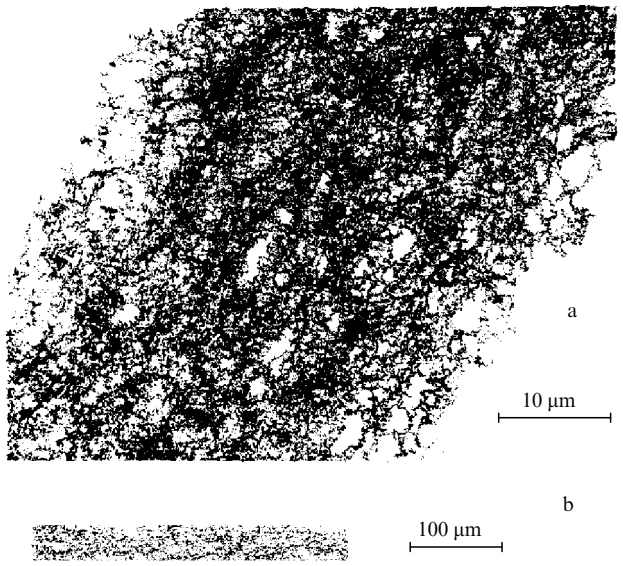

Figure 14. Portion of a fractal fiber cut out along (a) and across (b) of the fiber [193].

fractal fibers [193, 194] (Fig. 14). This phenomenon results from the interaction of dipole momenta of joining aggregates, which are induced by an external electric field. Subsequent joining of fractal fibers to one another leads to formation of fractal tangles [195] which are interwoven fibers having a specific structure. Thus, external fields influence the character of growth of fractal aggregates and can lead to formation of various structures.

It is important that electric fields highly accelerate the process of the joining of fractal aggregates to macroscopic structures. Since fractal aggregates are large compared with atomic particles, the role of induced dipole momenta in their interaction is stronger than that for atomic particles. Moreover, the structure of a growing system of fractal aggregates also varies under the action of an external field, and fractal fibres of joining fractal aggregates are ultimately formed instead of an isotropic aerogel. Indeed, chain structures formed at the first stage of association of fractal aggregates are stretched along the field, and new fractal aggregates with induced dipole moments join the endings of this chain [196]. Setting aside details of the growth process for the fiber structure of fractal aggregates, we give an estimate of a typical time for this process [31]:

$$\tau_1 \sim \frac{3\eta \ln (l/a)}{a^3 E^2 N}\,, \tag{6.28}$$

and this process proceeds in an electric field with strength E. Here, $l \sim 1$ cm is the structure length, $a \approx 40$ nm is the typical radius of monomers, N is the number density of monomers, and η is the viscosity of a buffer gas. Running the process at room temperature, atmospheric pressure, and a typical electric field strength of $E = 100$ V cm^{-1}, we obtain $\tau_1 \sim 20$ s for the above example of combustion of methane and SiH_4 in atmospheric air. As is seen, an electric field accelerates the joining of fractal aggregates to macroscopic structures and leads to the formation of fiber-like structures.

In conclusion, we note that the fiber-like structures of aerosols are known in aerosol physics as chain aggregates [152, 162]. Moreover, the connection between chain aggregates and electric fields is well known. The classical example of this is combustion of a magnesium band in air [197, 198] that leads to the formation of spherical aerosols consisting of magnesium oxides, whereas aerosols formed in smoke as a result of the same process in arc discharge have the fiber shape.

6.5 Coalescence

Coalescence is one of the mechanisms of cluster growth (see Fig. 10). This process results from the interaction of clusters with a parent vapor and is also known as Ostwald ripening [199, 200]. In this case, clusters are in equilibrium with a parent gas or vapor, i.e., the number of evaporated atoms from the cluster surface per unit time is equal to the number of free atoms attached to the cluster surface per unit time. However, the rate of atom evaporation is higher than the rate of atom attachment for small clusters, while for large clusters the inverse relation is fulfilled between the rates of atom attachment and atom evaporation. As a result, large clusters grow, while small clusters evaporate. Correspondingly, the average cluster size increases as a result of coalescence.

In reality, the diffusion and kinetic regimes of coalescence relate to different physical processes. Indeed, the diffusion regime describes the growth of grains in solid solutions. On the basis of this process, the classic theory of coalescence [201–203] was developed. Though the understanding of the growth process of clusters as a result of coalescence relates to the diffusion regime of grain growth in a solid solution [204, 205], a more convenient interpretation of this mechanism of cluster growth relates to the kinetic regime of cluster growth in a cluster plasma [58], and we will analyze below this very mechanism of coalescence. It should also be noted that, under equilibrium conditions, coagulation is a slow process connecting with cluster growth through cluster interaction with a gas component in the processes of cluster evaporation and attachment of free atoms to clusters. At a given temperature, clusters are found almost in equilibrium with a parent vapor, i.e., the number of events of cluster evaporation per unit time almost coincides with a number of atom attachments to clusters per unit time. A temperature variation then leads to displacement or disturbance of this equilibrium. Since the evaporation rate sharply depends on the temperature, a small temperature gradient in a gaseous system with clusters and their vapor leads to developing an instability (the cluster instability in the case of a cluster plasma [206]). As a result of this instability, a weak temperature gradient causes the diffusion flow of metal atoms, and in the end this leads to a transfer of all the metal to a cold region where it is present in the form of clusters.

For description of the coalescence process, we consider, as before, metal clusters injected into a buffer gas, and we characterize their amount by the concentration c_b of metal bound atoms. At a given temperature of a buffer gas, clusters evaporate and form a metal vapor of free metal atoms. Further, evaporation processes are accompanied by the attachment processes of free atoms to cluster surfaces, and these processes are equalized in the end. Denoting the concentration of free metal atoms in a buffer gas by c_m, we assume that $c_b \gg c_m$, i.e., the metal clusters are a large reservoir for free metal atoms. Coalescence proceeds with a weak disturbance of the equilibrium between free and bound atoms.

Let us consider the above equilibrium from the standpoint of an individual cluster, where formula (4.8) gives the

equilibrium number density of free atoms for this cluster. This equilibrium number density of free atoms is different depending on the cluster size, and the equilibrium between processes of atom evaporation and atom attachment is established for clusters of a definite size, so that for clusters of neighboring sizes this balance is disturbed weakly, leading in the end to cluster growth. Let us introduce a narrow size distribution function f_n of clusters:

$$f_n = \frac{N_{\rm cl}}{\sqrt{2\pi}\Delta} \exp\left[-\frac{(n-n_0)^2}{2\Delta^2}\right], \quad \Delta \ll n_0\,, \tag{6.29}$$

so that, by definition, $f_n\,{\rm d}n$ is the number density of clusters consisting of atoms with a number between n and $n+{\rm d}n$, and $N_{\rm cl}$ is the number density of clusters. We assume the width Δ of the size distribution function of clusters to be small compared with the average number n_0 of cluster atoms. The number of atoms attaching to clusters per unit volume and per unit time is expressed as

$$J = \int_0^\infty N_{\rm m} k_0 n^{2/3} f_n\,{\rm d}n = N_{\rm cl} N_{\rm m} k_0 n_0^{2/3} = N_{\rm b} N_{\rm m} k_0 n_0^{-1/3}\,,$$

and it is equal to the number of atoms evaporated from clusters per unit volume and per unit time.

Clusters may be divided into two groups, so that the first group includes those with the number of atoms above n_0, and the second group contains clusters where the number of atoms is below n_0. The difference in the rates of cluster evaporation and atom attachment to clusters has a different sign for the clusters of these groups, and is given by

$$\Delta J = \int_0^{n_0} N_{\rm m} k_0 n^{2/3} f_n\,{\rm d}n = \int_0^{n_0} N_{\rm m} k_0\,\frac{2(n_0-n)}{3n_0^{1/3}} f_n\,{\rm d}n$$
$$= N_{\rm cl} N_{\rm m} k_0\,\frac{2\sqrt{2}\Delta}{3\sqrt{\pi}\,n_0^{1/3}}\,.$$

Exactly this difference determines the rate of variation of the average cluster size. It is relatively small, so that

$$\frac{\Delta J}{J} = \frac{\sqrt{2}}{3\sqrt{\pi}}\,\frac{\Delta}{n_0}\,. \tag{6.30}$$

Based on these results, we determine the rate of an increase of the average cluster size. The processes for clusters of each group lead to an increase in the average cluster size by a value on the order of Δ, and the equation for the average cluster size $\overline{n}$ has the form

$$\frac{{\rm d}\overline{n}}{{\rm d}t} \sim \Delta\,\frac{\Delta J}{N_{\rm b}} \sim \frac{\Delta^2}{n_0^{4/3}}\,N_{\rm m} k_0\,,$$

since the rate of atom attachment to clusters (the number of attaching atoms per unit volume and per unit time) is $J \sim N_{\rm b} N_{\rm m} k_0 n_0^{-1/3}$. The coalescence process is an automodel one [204, 205], i.e., the size distribution function of clusters within some time after the beginning of the process becomes independent of the initial conditions. This also means that the parameters of the distribution function, its width Δ in this case, depend on the process character. One can connect the width of the distribution function with a random delay or acceleration of the evaporation process or the process of atom attachment to clusters. Therefore, $\Delta^2 = n_0$, and the equation of cluster growth in the kinetic regime takes the form

$$\frac{{\rm d}\overline{n}}{{\rm d}t} \sim N_{\rm m} k_0 n_0^{-1/3}\,. \tag{6.31}$$

As is seen, the rate of growth of the average cluster size at coalescence is proportional to the number density of free atoms through which the coalescence process is realized.

In the transition from the kinetic regime to the diffusion regime of coalescence, it is necessary, as usual, to replace the rate constant of atomic attachment to a cluster, $k_0 n^{2/3}$, according to formula (2.5) for the kinetic regime of the process, by its value $4\pi D_{\rm m} r_0$ for the diffusion regime in accordance with formula (2.8). As a result, the rate of the cluster size growth is found to be

$$\frac{{\rm d}\overline{n}}{{\rm d}t} \sim 4\pi D_{\rm m} r_{\rm W} N_{\rm m} n_0^{-2/3}\,. \tag{6.32}$$

6.6 Method of molecular dynamics in nucleation processes

We were based above on the analytical methods for the processes of nucleation and cluster growth. This group of processes relates to particle transitions from free to bound states. One can expect that computer methods are useful for the analysis of these problems and, primarily, the method of molecular dynamics, on the basis of which by putting a certain interaction potential of atomic particles one can follow the evolution of an ensemble of these atomic particles. Important results for some aspects of cluster physics have been obtained on the basis of the molecular dynamics method. In particular, phase coexistence was early analyzed in the cluster phase transition discovered in computer simulation of Lennard–Jones clusters by the method of molecular dynamics [207, 208]. Note also the study of hot liquid Lennard–Jones clusters by the method of molecular dynamics [209–211], which exhibits that the structure of large liquid clusters differs from that constructed on the basis of assumptions of classical thermodynamics [212–216].

One can add to this inference that there now exist computer codes (see, for example, Refs [217–219]) which allow one to use the method of molecular dynamics for certain problems. This makes the method of molecular dynamics to be available just like analytical methods. But just as with the use of analytical formulas, it is necessary in computer simulations to understand the problem under consideration from the standpoint of computer calculations, and this gives some requirements to the qualifications of the scientist. A formal use of computer methods may lead to contradictions. Let us analyze from this standpoint the rates of nucleation of an atomic vapor by the method of molecular dynamics [220–224].

The problem with computer simulations of nucleation processes which, due to their nature, correspond to transitions from a free state to a bound state of an atomic system or, on the contrary, from a bound state to a free state, is concerned with the large statistical weight of states of a continuous spectrum, which leads to different time scales for processes in this atomic system. In order to partially overcome difficulties with the simultaneous numerical analysis of these processes, a high density of the vapor and a small cell size are used in direct calculations of the nucleation rate for a supersaturated vapor located in a buffer gas, and this leads to unreal parameters of a nucleating vapor and to additional errors in the computer model. For example, nucleation of germanium atoms was investigated in Ref. [223] using 8000 atoms, and the ratio of the number of argon atoms to the number of germanium atoms varied from 1 to 5; these atoms were located in a cell with a linear size from 15 up to 60 nm.

Setting aside the choice of the interaction potential between atoms, we will analyze this calculation from the standpoint of the results obtained. If we use model (6.1) for this calculation, choosing in accordance with the parameters used a cell size of 20 nm, a buffer gas temperature of 300 K, and the ratio of the number of argon atoms in a cell to the number of germanium atoms to be 1, we find the value of parameter (6.2) to be $G = 14$. This allows us to use the model (6.1) for this process, and according to formulas (6.3) a time of cluster formation is $\tau_{\rm cl} = 1.5 \times 10^{-10}$ s, the average cluster size is about $\overline{n} = 3$ at the end of the nucleation process, and the maximum cluster size according to formula (6.3) is 9. According to computer calculations, the nucleation time $\tau_{\rm cl} = 6.3 \times 10^{-10}$ s, the average cluster size at the end of the process is $\overline{n} = 5$, and the maximum cluster size equals 36. One can connect this difference in results to the nonuniformity in the system under consideration because the number density of atoms under given conditions is 1×10^{21} cm^{-3}, i.e., the partial pressure of germanium vapor at the early stage of the process reaches 30 atm, which corresponds to unreal conditions.

Thus, the basic lack of calculations of the nucleation rate for an atomic vapor located in a buffer gas by methods of molecular dynamics consists in an unreal high initial pressure of the vapor, where other mechanisms may be responsible for nucleation. For example, in paper [224] the initial pressure of the copper vapor was 5.2–61 atm, while the saturated vapor pressure at the melting point $T_{\rm m} = 1358$ K of copper is 3.6×10^{-7} atm [164], and it is impossible to reach the initial parameters of the calculation. On the other hand, new mechanisms of nucleation are realized at high pressures, especially the thermal mechanism of nucleation, so the transfer of the results for high pressures to those at low pressures that have a practical interest leads to contradictions. Therefore, existing calculations of nucleation processes by methods of molecular dynamics cannot be used for modeling real processes.

This conclusion cannot be considered as a lack of computer simulations in comparison with analytical methods. Computer methods are a fine instrument and its using must be caused, in the first place, by an understanding of the physical processes under consideration, whereas the formal application of numerical simulations can lead to results which are not connected with reality. We obtain the same result if we apply wrong analytical formulas or analytical methods outside the validity of certain physical processes. The fact that the understanding of the principal aspects of cluster physics is bound to computer simulation is corroboration of the importance of numerical calculations.

7. Conclusions

Clusters as a system of bound atoms or molecules of nanometer sizes differ from small particles of micrometer sizes. This difference consists both in the principal role of cluster magic numbers and in the impossibility of keeping clusters in the form of a powder. In this case, contact between neighboring clusters takes place in a relatively large area and leads to the formation of chemical bonds between these clusters, which, in turn, is accompanied by a loss of initial cluster properties. In contrast, micron-sized particles related to certain materials or treated in a certain manner may be kept in the form of a powder [225]. Clusters exist either in the form of cluster beams or in a buffer gas.

In spite of the principal difference between clusters and microparticles, their behavior in a buffer gas is similar. Indeed, the interaction of clusters or microparticles with gas atoms or molecules proceeds in a narrow region on the order of atomic sizes near their surface, i.e., the size of the interaction region is small compared to the size of the cluster or microparticle. This allows us to use the same model for the interaction of clusters and small particles with atomic particles of a surrounding gas and, in this manner, to join the processes involving clusters and microparticles.

Experience in the analysis of these processes exhibits the existence of two mechanisms for these processes, depending on the relation between the mean free path of atomic particles under consideration in a surrounding gas (or the typical distance between active particles) and the size of the cluster or small particle. The latter size does not always coincides with the cluster or microparticle size. In particular, it is necessary to change the cluster radius by an average distance between attaching atoms in the case of atom attachment to a cluster. This gives additional mechanisms for processes involving clusters and small particles and requires the analysis of their criteria.

Thus, in analyzing the processes involving clusters and small particles in a buffer gas, one can extract two principally opposite regimes of these processes: kinetic and diffusion, depending on the relation between the mean free path of atoms or molecules in a buffer gas and the radius of the cluster or small particle (or between similar parameters of the size dimensionality). The free cluster motion takes place in the kinetic regime, whereas the diffusive motion of clusters proceeds in the diffusion regime. However, this dividing is insufficient for some processes involving clusters or small particles. For example, in the case of particle charging in an ionized gas, the mean free paths of electrons and ions may be different, and this can lead to additional regimes of charging of clusters and small particles. Next, a charged particle in a rarefied gas is surrounded by an ionic coat consisting of trapped and free ions, and a size of this coat may remarkably exceed the particle radius, so that this provides additional possibilities for the regimes of charging of clusters and small particles. In the case of cluster coalescence, the character of cluster approach depends on the cluster mean free path with respect to a variation of the cluster velocity, motion direction, and other parameters of the size dimensionality. This all testifies to the variety of regimes of processes involving clusters or small particles due to their interaction with a surrounding buffer or ionized gas, and it requires a careful analysis of the regimes of this interaction in studying the corresponding processes.

References

1. Smalley R E *Laser Chem.* **2** 167 (1983)
2. Hopkins J B et al. *J. Chem. Phys.* **78** 1627 (1983)
3. Yang S T et al. *Chem. Phys. Lett.* **139** 233 (1987)
4. Cheshnovsky O et al. *Rev. Sci. Instrum.* **58** 2131 (1987)
5. Milany P, de Heer W A *Rev. Sci. Instrum.* **61** 1835 (1990)
6. Haberland H et al. *J. Vac. Sci. Technol. A* **10** 3266 (1992)
7. Haberland H et al. *Phys. Rev. Lett.* **69** 3212 (1992)
8. Haberland H et al. *Mater. Sci. Engin. B* **19** 31 (1993)
9. Haberland H et al. *Z. Phys. D* **26** 8 (1993)
10. Haberland H et al. *J. Vac. Sci. Technol. A* **12** 2925 (1994)
11. Kashtanov P V, Smirnov B M, Hippler R *Usp. Fiz. Nauk* **177** 473 (2007) [*Phys. Usp.* **50** 455 (2007)]
12. Smirnov B M *Usp. Fiz. Nauk* **167** 1169 (1997) [*Phys. Usp.* **40** 1117 (1997)

13. Smirnov B M *Usp. Fiz. Nauk* **172** 609 (2003) [*Phys. Usp.* **46** 589 (2003)]
14. Hagena O F *Surf. Sci.* **106** 101 (1981)
15. Gspann J *Z. Phys. D* **3** 143 (1986)
16. Hagena O F *Z. Phys. D* **4** 291 (1987)
17. Hagena O F *Z. Phys. D* **17** 157 (1990)
18. Hagena O F *Z. Phys. D* **20** 425 (1991)
19. Hagena O F *Rev. Sci. Instrum.* **63** 2374 (1992)
20. Rao A K, Whitby K T *J. Aerosol Sci.* **9** 77 (1978)
21. Reist P C *Introduction to Aerosol Science* (New York: Macmillan Publ. Co., 1984)
22. White H J *Industrial Electrostatic Precipitation* (Reading, Mass.: Addison-Wesley, 1963)
23. Oglesby S (Jr.), Nichols G B *Electrostatic Precipitation* (New York: M. Decker, 1978)
24. Parker K P (Ed.) *Applied Electrostatic Precipitation* (London: Blackie, 1997)
25. Lakhno V D *Klastery v Fizike, Khimii i Biologii* (Clusters in Physics, Chemistry, and Biology) (Moscow-Izhevsk: R&C Dynamics, 2001)
26. Mott-Smith H M, Langmuir I *Phys. Rev.* **28** 727 (1926)
27. Shun'ko E V *Langmuir Probe in Theory and Practice* (Boca Raton: Brown Walker Press, 2008)
28. Henniker Scientific, http://www.henniker-scientific.com
29. Al'pert Ya L, Gurevich A V, Pitaevskii L P *Usp. Fiz. Nauk* **79** 23 (1963) [*Sov. Phys. Usp.* **6** 13(1963)]
30. Al'pert Ya L, Gurevich A V, Pitaevskii L P *Iskusstvennye Sputniki v Razrezhennoi Plazme* (Artificial Satellites in Rarefied Plasma) (Moscow: Nauka, 1964) [Translated into English: *Space Physics with Artificial Satellites* (New York: Consultants Bureau, 1965)]
31. Smirnov B M *Clusters and Small Particles*: *in Gases and Plasmas* (New York: Springer, 2000)
32. Eletskii A V, Palkina L A, Smirnov B M *Yavleniya Perenosa v Slaboionizovannoi Plazme* (Transport Phenomena in a Weakly Ionized Plasma) (Moscow: Atomizdat, 1975)
33. Echt O, Sattler K, Recknagel E *Phys. Rev. Lett.* **94** 54 (1981)
34. Miehle W et al. *J. Chem. Phys.* **91** 5940 (1989)
35. Martin T P et al. *Chem. Phys. Lett.* **176** 343 (1991)
36. Martin T P et al. *Chem. Phys. Lett.* **172** 209 (1990)
37. Schmidt M et al. *Phys. Rev. Lett.* **79** 99 (1997)
38. Schmidt M et al. *Nature* **393** 238 (1998)
39. Hoare M R, Pal P *Adv. Phys.* **20** 161 (1971)
40. Hoare M R, Pal P *Adv. Phys.* **24** 645 (1975)
41. Hoare M R *Adv. Chem. Phys.* **40** 49 (1979)
42. Stillinger F H, Weber T A *Phys. Rev. A* **25** 978 (1982)
43. Stillinger F H, Weber T A *Phys. Rev. A* **28** 2408 (1983)
44. Wales D J et al. *Adv. Chem. Phys.* **115** 1 (2000)
45. Wales D J *Energy Landscapes* (Cambridge: Cambridge Univ. Press, 2003)
46. Jellinek J, Beck T L, Berry R S *J. Chem. Phys.* **84** 2783 (1986)
47. Davis H L, Jellinek J, Berry R S *J. Chem. Phys.* **86** 6456 (1987)
48. Honeycutt J D, Andersen H C *J. Phys. Chem.* **91** 4950 (1987)
49. Berry R S, Smirnov B M *Usp. Fiz. Nauk* **179** 147 (2009) [*Phys. Usp.* **52** 137(2009)]
50. Smirnov B M *Principles of Statistical Physics* (Weinheim: Wiley-VCH, 2006)
51. Bohr N *Nature* **137** 344 (1936)
52. Bohr N, Kalckar F *Kgl. Danske Vid. Selskab. Math. Fys. Med.* **14** 1 (1937)
53. Gamow G *Structure of Atomic Nuclei and Nuclear Transformations* (Oxford: The Clarendon Press, 1937)
54. Bohr N *Nature* **143** 330 (1939)
55. Bohr N, Wheeler J A *Phys. Rev.* **56** 426 (1939)
56. Wigner E P, Seitz F *Phys. Rev.* **46** 509 (1934)
57. Wigner E *Phys. Rev.* **46** 1002 (1934)
58. Smirnov B M *Cluster Processes in Gases and Plasmas* (Weinheim: Wiley-VCH, 2010)
59. Smirnov B M *Reference Data on Atomic Physics and Atomic Processes* (New York: Springer, 2008)
60. Maxwell J C *Philos. Mag.* **19** 19 (1860)
61. Maxwell J C *Philos. Mag.* **20** 21 (1860)
62. Maxwell J C *Theory of Heat* (London: Longmans, Green and Co., 1871)
63. Bird G A *Molecular Gas Dynamics* (Oxford: Clarendon Press, 1976)
64. Hansen J P, McDonald I R *Theory of Simple Liquids* (London: Academic Press, 1986)
65. Wilson J R *Metallurg. Rev.* **10** 381 (1965) [Translated into Russian: *Struktura Zhidkikh Metallov i Splavov* (Moscow: Metallurgiya, 1972)]
66. Sutton A P, Chen J *Philos. Mag. Lett.* **61** 139 (1990)
67. Chadi D J *Phys. Rev. B* **19** 2074 (1979)
68. Sutton A P et al. *J. Phys. C* **21** 35 (1988)
69. Hohenberg P, Kohn W *Phys. Rev.* **136** B864 (1964)
70. Kohn W, Sham L J *Phys. Rev.* **140** A1133 (1965)
71. Suzdalev I P *Nanotechnologiya*: *Fiziko-Khimiya Nanoklasterov, Nanostruktur i Nanomaterialov* (Nanotechnology: Physical Chemistry of Nanoclusters, Nanostructures, and Nanomaterials) (Moscow: KomKniga, 2006)
72. Makarov G N *Usp. Fiz. Nauk* **178** 337 (2008) [*Phys. Usp.* **51** 319 (2008)]
73. Makarov G N *Usp. Fiz. Nauk* **180** 185 (2010) [*Phys. Usp.* **53** 179 (2010)]
74. Smoluchowski M V *Phys. Z.* **17** 557 (1916)
75. Chapman S, Cowling T G *The Mathematical Theory of Non-uniform Gases* (Cambridge: Univ. Press, 1952)
76. Ferziger J H, Kaper H G *Mathematical Theory of Transport Processes in Gases* (Amsterdam: North-Holland, 1972)
77. Lifshitz E M, Pitaevskii L P *Fizicheskaya Kinetika* (Physical Kinetics) (Moscow: Nauka, 1979) [Translated into English (Oxford: Pergamon Press, 1981)]
78. Stokes G G *Trans. Cambr. Philos. Soc.* **9** 8 (1851)
79. Landau L D, Lifshitz E M *Gidrodinamika* (Fluid Mechanics) (Moscow: Nauka, 1986) [Translated into English (Oxford: Pergamon Press, 1987)]
80. Smirnov B M *Dokl. Akad. Nauk SSSR* **168** 322 (1966) [*Sov. Phys. Dokl.* **11** 429 (1966)]
81. Einstein A *Ann. Physik* **322** 549 (1905)
82. Einstein A *Ann. Physik* **324** 371 (1906)
83. Einstein A *Z. Electrochem. Angew. Phys. Chem.* **14** 235 (1908)
84. Nernst W *Z. Phys. Chem.* **2** 613 (1888)
85. Townsend J S *Philos. Trans. R. Soc. Lond. A* **193** 129 (1900)
86. Townsend J S, Bailey V A *Philos. Trans. A* **195** 259 (1900)
87. Huxley L G H, Crompton R W *The Diffusion and Drift of Electrons in Gases* (New York: Wiley, 1974)
88. McDaniel E W, Mason E A *The Mobility and Diffusion of Ions in Gases* (New York: Wiley, 1973)
89. Smirnov B M *Usp. Fiz. Nauk* **170** 495 (2000) [*Phys. Usp.* **43** 453 (2000)]
90. Smirnov B M *Physics of Ionized Gases* (New York: Wiley, 2001)
91. Ino S *J. Phys. Soc. Jpn.* **27** 941 (1969)
92. Vargaftik N B *Spravochnik po Teplofizicheskim Svoistvam Gazov i Zhidkostei* (Tables on the Thermophysical Properties of Liquids and Gases) (Moscow: Nauka, 1972) [Translated into English (Washington: Hemisphere Publ. Corp., 1975)]
93. Vargaftik N B et al. *Spravochnik po Teploprovodnosti Zhidkostei i Gazov* (Handbook of Thermal Conductivity of Liquids and Gases) (Moscow: Energoatomizdat, 1990) [Translated into English (Boca Raton: CRC Press, 1994)]
94. Shyjumon I et al. *Thin Solid Films* **500** 41 (2006)
95. Shukla P K, Mamun A A *Introduction to Dusty Plasma Physics* (Bristol: IOP Publ., 2002)
96. Shukla P K (Ed.) *Dust Plasma Interaction in Space* (Hauppauge, N.Y.: Nova Sci. Publ., 2002)
97. Fortov V E et al. *Usp. Fiz. Nauk* **174** 495 (2004) [*Phys. Usp.* **47** 447 (2004)]
98. Fortov V E, Iakubov I T, Khrapak A G *Physics of Strongly Coupled Plasma* (Oxford: Oxford Univ. Press, 2006)
99. Melzer A, Goree J, in *Low Temperature Plasmas* Vol. 1 (Eds R Hippler et al.) (Berlin: Wiley, 2008) p. 129
100. Hippler R, Kersten H, in *Low Temperature Plasmas* Vol. 2 (Eds R Hippler et al.) (Berlin: Wiley, 2008) p. 787
101. Fortov V E, Morfill G E (Eds) *Complex and Dusty Plasmas*: *from Laboratory to Space* (Boca Raton: CRC Press/Taylor and Francis, 2010)
102. Debye P, Hückel E *Phys. Z.* **24** 185 (1923)

103. Landau L D, Lifshitz E M *Statisticheskaya Fizika* (Statistical Physics) Vol. 1 (Moscow: Nauka, 1976) [Translated into English (Oxford: Pergamon Press, 1980)]
104. Landau L D, Lifshitz E M *Mekhanika* (Mechanics) (Moscow: Nauka, 1973) [Translated into English (Oxford: Pergamon Press, 1980)]
105. Birkhoff G D *Proc. Natl. Acad. Sci. USA* **17** 656 (1931)
106. v. Neumann J *Proc. Natl. Acad. Sci. USA* **18** 70 (1932)
107. v. Neumann J *Proc. Natl. Acad. Sci. USA* **18** 263 (1932)
108. Isihara A *Statistical Physics* (New York: Academic Press, 1971) [Translated into Russian (Moscow: Mir, 1973)]
109. Smirnov B M *Zh. Eksp. Teor. Fiz.* **137** 1195 (2010) [*JETP* **110** 1042 (2010)]
110. Smythe W R *Static and Dynamic Electricity* (New York: McGraw Hill, 1950) [Translated into Russian (Moscow: IL, 1954)]
111. Jackson J D *Classical Electrodynamics* (New York: Wiley, 1999) [Translated into Russian (Moscow: Mir, 1965)]
112. Holstein T *J. Phys. Chem.* **56** 832 (1952)
113. Smirnov B M *Usp. Fiz. Nauk* **170** 495 (2000) [*Phys. Usp.* **43** 453 (2000)]
114. Bernstein I B, Rabinowitz I N *Phys. Fluids* **2** 112 (1959)
115. Zaslavsky G M, Sagdeev R Z *Vvedenie v Nelineinuyu Fiziku*: *Ot Mayatnika do Turbulentnosti i Khaosa* (Introduction to Nonlinear Physics: From the Pendulum to Turbulence and Chaos) (Moscow: Nauka, 1988); *Nonlinear Physics: from the Pendulum to Turbulence and Chaos* (Chur: Harwood Acad. Publ., 1988)
116. Zobnin A V, Nefedov A P, Sinel'shchikov V A, Fortov V E *Zh. Eksp. Teor. Fiz.* **118** 554 (2000) [*JETP* **91** 483 (2000)]
117. Lampe M et al. *Phys. Rev. Lett.* **86** 5278 (2001)
118. Lampe M et al. *Phys. Scripta* **T98** 91 (2002)
119. Lampe M et al. *Phys. Plasmas* **10** 1500 (2003)
120. Bystrenko O, Zagorodny A *Phys. Rev. E* **67** 066403 (2003)
121. Sternovsky Z, Lampe M, Robertson S *IEEE Trans. Plasma Sci.* **32** 632 (2004)
122. Sukhinin G I, Fedoseev A V *Fiz. Plazmy* **33** 1117 (2007) [*Plasma Phys. Rep.* **33** 1023 (2007)]
123. Sukhinin G I et al. *Phys. Rev. E* **79** 036404 (2009)
124. Sukhinin G et al. *J. Phys. A Math. Theor.* **42** 214027 (2009)
125. Sena L A *Zh. Eksp. Teor. Fiz.* **16** 734 (1946)
126. Sena L A *Stolknoveniya Elektronov i Ionov s Atomami Gaza* (Collisions of Electrons and Ions with Gas Atoms) (Leningrad – Moscow: Gostekhizdat, 1948)
127. Smirnov B M *Physics of Atoms and Ions* (New York: Springer, 2003)
128. Hirschfelder J O, Curtiss Ch F, Bird R B *Molecular Theory of Gases and Liquids* (New York: Wiley, 1954)
129. Bliokh P, Sinitsin V, Yaroshenko V *Dusty and Self-Gravitational Plasmas in Space* (Dordrecht: Kluwer Acad. Publ., 1995)
130. Somov B V *Cosmic Plasma Physics* (Dordrecht: Kluwer Acad. Publ., 2000)
131. Meyer-Vernet N *Basics of the Solar Wind* (Cambridge: Cambridge Univ. Press, 2007)
132. Hundhausen A J, in *Introduction to Space Physics* (Eds M G Kivelson, C T Russell) (Cambridge: Cambridge Univ. Press, 1995) p. 91
133. Mendis D A, Rosenberg M *Annu. Rev. Astron. Astrophys.* **32** 419 (1994)
134. Bosh A S et al. *Icarus* **157** 57 (2002)
135. Morfill G E, Grün E, Johnson T V *J. Geophys. Res.* **88** 5573 (1983)
136. Dikarev V V *Astron. Astrophys.* **346** 1011 (1999)
137. Havnes O, Morfill G, Melandsø F *Icarus* **98** 141 (1992)
138. Matthews L S, Hyde T W *Adv. Space Res.* **33** 2292 (2004)
139. Srama R et al. *Planet. Space Sci.* **54** 967 (2006)
140. Porco C C et al. *Science* **311** 1393 (2006)
141. Wang Z et al. *Planet. Space Sci.* **54** 957 (2006)
142. Kurth W S et al. *Planet. Space Sci.* **54** 988 (2006)
143. Gan-Baruch Z et al. *J. Geophys. Res.* **99** 11063 (1994)
144. Comet West, http://www.solarviews.com/raw/comet/west.gif
145. Krishna Swamy K S *Physics of Comets* (Singapore: World Scientific, 1997)
146. Brandt J C, Chapman R D *Introduction to Comets* (Cambridge: Cambridge Univ. Press, 2004)
147. Mendis D A *Annu. Rev. Astron. Astrophys.* **26** 11 (1988)
148. Wright C S, Nelson G J *Icarus* **38** 123 (1979)
149. Meyer-Vernet N et al. *Astron. J.* **93** 474 (1987)
150. Vourlidas A et al. *Astrophys. J.* **668** L79 (2007)
151. Buffington A et al. *Astrophys. J.* **677** 798 (2008)
152. Fuks N A *Mekhanika Aerozolei* (The Mechanics of Aerosols) (Moscow: Izd. AN SSSR, 1955) [Translated into English (New York: Macmillan, 1964)]
153. Langevin P *Ann. Chim. Phys.* **5** 245 (1905)
154. Bryant P *J. Phys. D* **36** 2859 (2003)
155. Khrapak S A et al. *Phys. Rev. E* **72** 016406 (2005)
156. Khrapak S A et al. *Phys. Plasmas* **13** 052114 (2006)
157. D'yachkov L G et al. *Phys. Plasmas* **14** 042102 (2007)
158. Gatti M, Kortshagen U *Phys. Rev. E* **78** 046402 (2008)
159. Smirnov B M *Usp. Fiz. Nauk* **164** 665 (1994) [*Phys. Usp.* **37** 621 (1994)]
160. Smirnov B M, Strizhev A Yu *Phys. Scripta* **49** 615 (1994)
161. Smirnov B M, Shyjumon I, Hippler R *Phys. Scripta* **73** 288 (2006)
162. Green H L, Lane W R *Particulate Clouds*: *Dusts, Smokes, and Mists* (Princeton, N.J.: Van Nostrand, 1964)
163. Licht W *Air Pollution Control Engineering* (New York: M. Dekker, 1980)
164. Voloshchuk V M *Kineticheskaya Teoriya Koagulyatsii* (Kinetic Theory of Coagulation) (Leningrad: Gidrometeoizdat, 1984)
165. Smoluchowski M *Z. Phys. Chem.* **92** 129 (1918)
166. Rao B K, Smirnov B M *Phys. Scripta* **56** 439 (1997)
167. Rao B K, Smirnov B M *Mater. Phys. Mech.* **5** 1 (2002)
168. Mokhov A (Gröningen University, Holland) gives kindly "Typical parameters of a flame in combustion of methane and SiH_4"
169. Lide D R (Ed.) *Handbook of Chemistry and Physics* 86th ed. (London: CRC Press, 2003 – 2004)
170. Witten T A (Jr.), Sander L M *Phys. Rev. Lett.* **47** 1400 (1981)
171. Meakin P *Phys. Rev. Lett.* **51** 1119 (1983)
172. Kolb M, Botet R, Jullien R *Phys. Rev. Lett.* **51** 1123 (1983)
173. Avnir D (Ed.) *The Fractal Approach to Heterogeneous Chemistry*: *Surfaces, Colloids, Polymers* (Chichester: Wiley, 1989)
174. Vicsek T *Fractal Growth Phenomena* (Singapore: World Scientific, 1989)
175. Smirnov B M *Fizika Fraktal'nykh Klasterov* (Physics of Fractal Clusters) (Moscow: Nauka, 1991)
176. Gouyet J-F *Physics and Fractal Structures* (New York: Springer, 1996)
177. Nakayama T, Yakubo K *Fractal Concepts in Condensed Matter Physics* (Berlin: Springer, 2003)
178. Mandelbrot B B *The Fractal Geometry of Nature* (San Francisco: W.H. Freeman, 1982)
179. Feder J *Fractals* (New York: Plenum Press, 1988)
180. Smirnov B M *Phys. Rep.* **188** 1 (1990)
181. Meakin P *Phys. Rev. A* **29** 997 (1984)
182. Jullien R, Kolb M, Botet R *J. Physique Lett.* **45** L211 (1984)
183. Kolb M *Phys. Rev. Lett.* **53** 1653 (1984)
184. Botet R, Jullien R, Kolb M *Phys. Rev. A* **30** 2150 (1984)
185. Meakin P *J. Colloid Interface Sci.* **102** 491 (1984)
186. Kim S G, Brock J R *J. Colloid Interface Sci.* **116** 431 (1987)
187. Smirnov B M, in *Proc. 8th European Physics Conf., Trends in Physics* (Ed. F Pleiter) (Amsterdam: North-Holland, 1990) p. 84
188. Lushnikov A A, Pakhomov A V, Chernyaeva G A *Dokl. Akad. Nauk SSSR* **292** 86 (1987) [*Sov. Phys. Dokl.* **32** 45 (1987)]
189. Lushnikov A A, Maksimenko V V, Pakhomov A V *J. Aerosol Sci.* **20** 865 (1989)
190. Fricke J (Ed.) *Aerogels*: *Proc. of the First Intern. Symp., Germany, September 23 – 25, 1985* (Berlin: Springer-Verlag, 1986)
191. Smirnov B M *Usp. Fiz. Nauk* **152** 133 (1987) [*Sov. Phys. Usp.* **30** 420 (1987)]
192. Fricke J *Sci. Am.* **258** (5) 92 (1988)
193. Lushnikov A A, Negin A E, Pakhomov A V *Chem. Phys. Lett.* **175** 138 (1990)
194. Lushnikov A A et al. *Usp. Fiz. Nauk* **161** (2) 113 (1991) [*Sov. Phys. Usp.* **34** 160 (1991)]
195. Smirnov B M *Usp. Fiz. Nauk* **161** (8) 141 (1991) [*Sov. Phys. Usp.* **34** 711 (1991)]
196. Smirnov B M *Problema Sharovoi Molnii* (Problem of Ball Lightning) (Moscow: Nauka, 1988)

197. Whytlaw-Gray R, Patterson H S *Smoke*: *a Study of Aeral Disperse Systems* (London: E.Arnold, 1932) [Translated into Russian (Moscow – Leningrad: Goskhimtekhizdat, 1934)]
198. Beischer D *Z. Electrochem.* **44** 375 (1938)
199. Ostwald W *Z. Phys. Chem.* **22** 289 (1897)
200. Ostwald W *Z. Phys. Chem.* **34** 495 (1900)
201. Lifshitz I M, Slezov V V *Zh. Eksp. Teor. Fiz.* **35** 479 (1958) [*Sov. Phys. JETP* **8** 331 (1959)]
202. Lifshitz I M, Slezov V V *Fiz. Tver. Tela* **1** 1401 (1959)
203. Lifshitz I M, Slezov V V *J. Phys. Chem. Sol.* **19** 35 (1961)
204. Lifshitz E M, Pitaevskii L P *Statisticheskaya Fizika* (Statistical Physics) Pt. 2 (Moscow: Nauka, 1978) [Translated into English: Vol. 2 (Oxford: Pergamon Press, 1980)]
205. Slezov V V, Sagalovich V V *Usp. Fiz. Nauk* **151** 67 (1987) [*Sov. Phys. Usp.* **30** 23 (1987)]
206. Smirnov B M *Phys. Scripta* **58** 363 (1998)
207. Berry R S et al. *Adv. Chem. Phys.* **70** 75 (1988)
208. Berry R S *Chem. Rev.* **93** 2379 (1993)
209. Zhukhovitskii D I *J. Chem. Phys.* **103** 9401 (1995)
210. Zhukhovitskii D I *J. Chem. Phys.* **110** 7770 (1999)
211. Zhukhovitskii D I *Zh. Eksp. Teor. Fiz.* **121** 396 (2002) [*JETP* **94** 336 (2002)]
212. Gibbs J W *The Collected Works* (New York: Longmans and Green and Co., 1928)
213. Frenkel J *Kineticheskaya Teoriya Zhidkostei* (Kinetic Theory of Liquids) (Moscow – Leningrad: Izd. AN SSSR, 1945) [Translated into English (Oxford: The Clarendon Press, 1946)]
214. Egelstaff P A *An Introduction To the Liquid State* (London: Academic Press, 1967)
215. Ubbelohde A R *The Molten State of Matter* (Chichester: Wiley, 1978)
216. Baidakov V G *Mezhfaznaya Granitsa Prostykh Klassicheskikh i Kvantovykh Zhidkostei* (Interface of Simple Classical and Quantum Liquids) (Ekaterinburg: Nauka, 1994)
217. Hypercube, Inc., http://www.hyper.com/
218. Visual Molecular Dynamics, http://www.ks.uiuc.edu/Research/vmd/
219. LAMMPS Mol. Dynamics Simulator, http://lammps.sandia.gov/
220. Krasnochtchekov P, Averback R S *J. Chem. Phys.* **122** 044319 (2005)
221. Lümmen N, Kraska T *Nanotechnol.* **16** 2870 (2005)
222. Lümmen N, Kraska T *Phys. Rev. B* **71** 205403 (2005)
223. Krasnochtchekov P et al. *J. Chem. Phys.* **123** 154314 (2005)
224. Kesälä E, Kuronen A, Nordlund K *Phys. Rev. B* **75** 174121 (2007)
225. Morokhov I D, Trusov L I, Lapovok V N *Fizicheskie Yavleniya v Ul'tradispersnykh Sredakh* (Physical Phenomena in Ultra-Disperse Media) (Moscow: Energoatomizdat, 1984)